PNL-7648
UC-802

2F

Assessment of the Hydrologic Impact of Extending Exploratory Shafts into the Calico Hills Nonwelded Tuff Unit at Yucca Mountain, Nevada

W. E. Nichols
M. D. Freshley
M. L. Rockhold

March 1991

Prepared for the U.S. Department of Energy
under Contract DE-AC06-76RLO 1830

Pacific Northwest Laboratory
Operated for the U.S. Department of Energy
by Battelle Memorial Institute

Battelle

PNL-7648

DISCLAIMER

PACIFIC NORTHWEST LABORATORY
operated by
BATTELLE MEMORIAL INSTITUTE
for the
UNITED STATES DEPARTMENT OF ENERGY
under Contract DE-AC06-76RLO 1830

Printed in the United States of America

Available to DOE and DOE contractors from the Office of Scientific and Technical Information, P.O. Box 62, Oak Ridge, TN 37831; prices available from (615) 576-8401. FTS 626-8401.

Available to the public from the National Technical Information Service, U.S. Department of Commerce, 5285 Port Royal Rd., Springfield, VA 22161.

PNL-7648
UC-802

ASSESSMENT OF THE HYDROLOGIC IMPACT OF EXTENDING EXPLORATORY SHAFTS INTO THE CALICO HILLS NONWELDED TUFF UNIT AT YUCCA MOUNTAIN, NEVADA

W. E. Nichols
M. D. Freshley
M. L. Rockhold

March 1991

Prepared for
the U.S. Department of Energy
under Contract DE-AC06-76RLO 1830

Pacific Northwest Laboratory
Richland, Washington 99352

EXECUTIVE SUMMARY

The U.S. Department of Energy is conducting studies for characterization of Yucca Mountain, Nevada, as a potential site for the nation's high-level nuclear waste repository. The plans for characterization include extending exploratory shafts into the Calico Hills nonwelded (CHn) unit of volcanic tuff at Yucca Mountain. Concerns have been raised that extending the exploratory shaft(s) will compromise the integrity of the CHn unit, which is considered a natural barrier to the migration of radionuclides to the water table. This characterization activity has been deferred, and a risk/benefit analysis is being conducted to recommend a strategy for characterizing the CHn unit. The risks associated with this activity are the potential adverse impacts to site performance, while the benefits would be realized as improved confidence in predictions of site performance.

To support the risk/benefit analysis, Pacific Northwest Laboratory[a] performed several numerical simulations of the CHn unit at the spatial scale of the hydrologic disturbance caused by the presence of a vertical shaft. The conceptual model for our study is based on the stratigraphy of borehole USW-G4. Only the CHn unit was considered, and was separated into vitric and zeolitic layers, based on lithologic characteristics. The shaft was assumed to extend into the CHn unit to a point 50 m above the water table. A modified permeability zone (MPZ) around the shaft was included in the model to account for changes in rock mass permeability that result from shaft construction. Coarse material (crushed tuff) with hydraulic properties of gravelly sand was assumed as the backfill material for the shaft. The region around the exploratory shaft extending into the CHn unit was represented as a three-dimensional, radially symmetric region, and was modeled with the PORFLO-3©[b] computer code.

Several cases were simulated to test different aspects of the conceptual model. The response of the flow system to changes in the conceptual model was shown using graphs of hydraulic head, saturation, and streamlines. Ratios of travel time and outflow arrival curves were also used to compare between undisturbed conditions and conditions after shaft extension. In general, the results strongly depend on the hydraulic properties assumed to represent the backfill material. Therefore, it is important to select and specify backfill material with hydraulic properties that minimize the potential influences of the shaft and the MPZ. Impacts of the backfilled shaft and MPZ were also amplified by heterogeneities present in the conceptual model in the form of stratigraphic layers of differing properties and by increases in the recharge rate. The reduction in travel time across the CHn unit due to the presence of a shaft and MPZ ranged from

---

(a) Pacific Northwest Laboratory is operated for the U.S. Department of Energy by Battelle Memorial Institute.

(b) PORFLO-3© is copyrighted by Analytic and Computational Research, Incorporated, subject to the Limited Government License.

0% to approximately 58% under expected hydrologic conditions, compared to the undisturbed flow regime. However, no travel time predicted in this analysis was less than the 1000-yr minimum travel time required by regulations. The effects were restricted to the 80-m radius modeled. Therefore, the effects are expected to be small compared to the overall size of the potential repository. Furthermore, the presence of a shaft and MPZ produced only slight changes in outflow arrival curves compared to corresponding undisturbed conditions.

CONTENTS

FIGURES

TABLE

1.0 INTRODUCTION

1.1 BACKGROUND

The U.S. Department of Energy (DOE) is performing analyses to address an objection by the U.S. Nuclear Regulatory Commission to plans in the Consultation Draft of the Site Characterization Plan (DOE 1988a) for direct excavation of the Calico Hills nonwelded (CHn) unit within the repository exploration block at Yucca Mountain, Nevada (Figure 1.1). The excavation was planned as part of site characterization activities for the potential high-level nuclear waste repository at Yucca Mountain. This characterization activity has been deferred, pending the results of a risk/benefit analysis of alternative methods for obtaining needed characterization data from the CHn unit. The benefits from characterizing the CHn unit are generally related to obtaining information leading to improved confidence in predictions of site performance. The risks are generally associated with potential adverse impacts to site performance that result from excavation or other intrusion into the CHn unit.

The purpose of the risk/benefit analysis is to produce a recommendation to the Director, Regulatory and Site Evaluation Division, DOE/Yucca Mountain Site Characterization Project Office for a strategy for characterizing the CHn unit. The recommendation will describe characterization activities that are expected to provide the needed information while limiting adverse impacts to site performance to the extent practical. The recommendation is to be based on comparative analyses of alternative strategies generated from systematic review of characterization technologies. A working group was formed by DOE to conduct the risk/benefit analysis. The working group is responsible for developing a list of information needed to characterize the CHn unit, identifying characterization techniques that are appropriate for obtaining this information, proposing alternative characterization strategies, and performing comparative analyses to develop a recommendation for characterization of the unit. The approach and assumptions are to be clearly stated in documentation for the analyses.

The risk/benefit analysis was supported with scoping calculations to provide a quantitative evaluation of the impacts associated with different strategies. The working group responsible for the risk/benefit analysis requested that these scoping calculations be supported with more detailed performance assessments for evaluating impacts of different characterization activities. This report summarizes the results of these performance assessment analyses.

The performance assessment calculations proposed to support the risk/benefit analysis included a number of different analyses. The analyses included in this study were designed to provide 1) an estimate of the properties of the modified permeability zones (MPZs) around boreholes, shafts, drifts, and ramps in the nonwelded tuff and 2) an evaluation of the effects of the backfill materials and the MPZ on travel time by comparison with undisturbed areas.

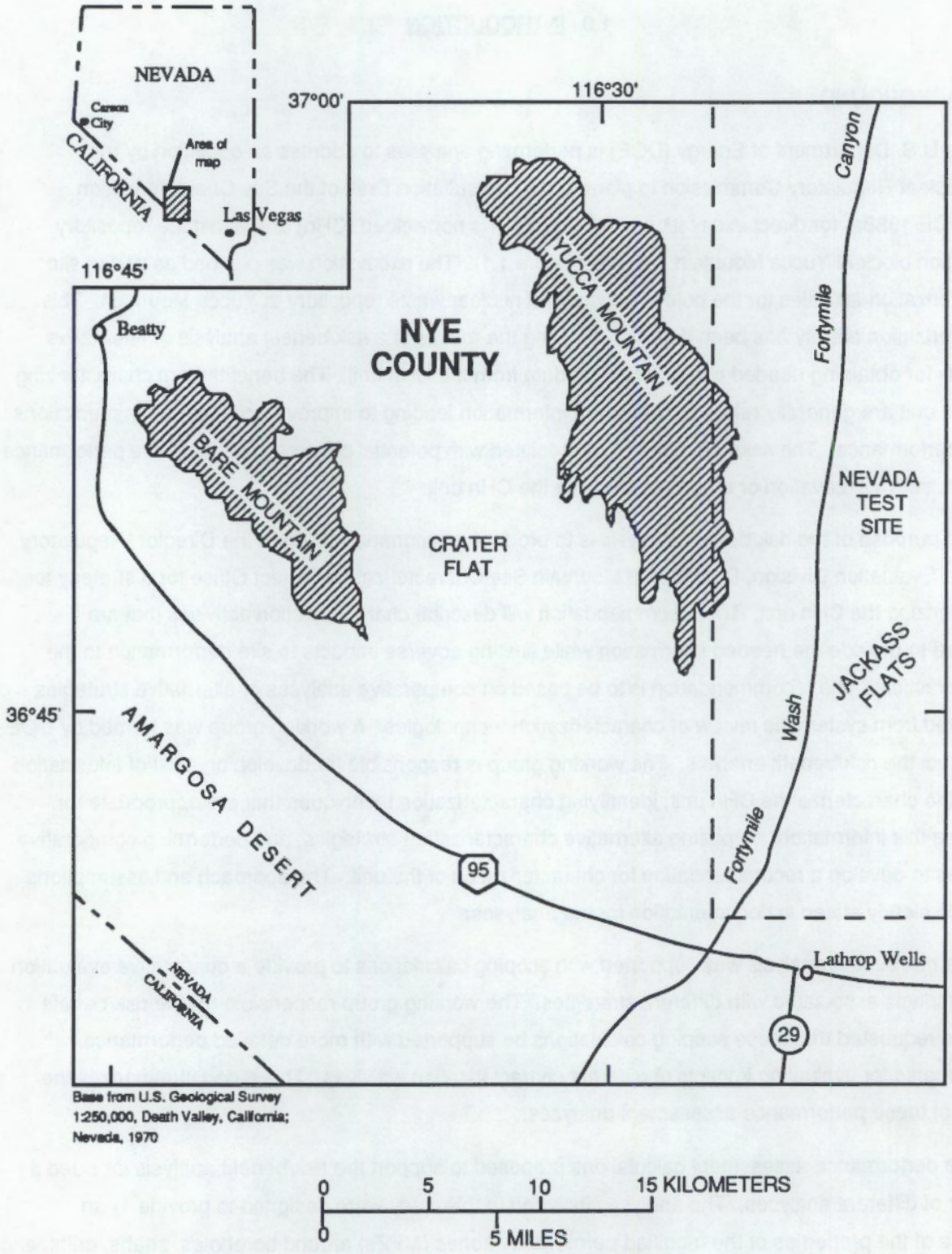

FIGURE 1.1. Physiographic Features of Yucca Mountain and Surrounding Region (modified from Montazer and Wilson 1984)

1.2 PREVIOUS ASSESSMENTS OF EXPLORATORY SHAFT FACILITY IMPACTS

Other researchers participating in the Yucca Mountain Project have investigated the effects of shafts and drifts on water flow through the mountain. The exploratory shaft facility is expected to be composed of shafts, inclined ramps, and drifts. Analyses have been conducted to evaluate the effects of these different construction features on expected performance of the potential repository at Yucca Mountain.

Relatively early in the investigation of Yucca Mountain as a potential repository site, Fernandez and Freshley (1984) and Freshley, Dove, and Fernandez (1985) investigated the effects of shafts and drifts on flow in the Topopah Spring welded unit in their development of concepts for sealing the potential repository. They used a model, based on the TRUST computer code, to perform preliminary calculations for different backfill materials under consideration for sealing the potential repository in the Topopah Spring welded unit. They did not evaluate the effects of MPZs surrounding drifts and shafts on their predicted flow fields. Freshley, Dove, and Fernandez (1985) found that coarse materials used for backfill, such as crushed tuff that was represented by hydraulic properties of coarse sand, performed more satisfactorily as a barrier to water flow through drifts and shafts than fine materials. Water flow into the drift was found to depend on the saturation level of the surrounding host rock. As the saturation increases, water flow into the drift increases. At very high saturations (98% to 99%), corresponding to a recharge rate at the upper boundary of the model of 0.4 mm yr^{-1}, the water inflow to the drift as a percent of the water flowing into the intercept area ranged from 0% to 17% (Fernandez and Freshley 1984). The intercept area is the width of the drift at the top boundary of the model.

In addition to the analyses of the repository drift, Freshley, Dove, and Fernandez (1985) also evaluated the impacts of a vertical shaft that intersects a geologic contact between volcanic tuff units. Different combinations of welded and nonwelded tuff units were used to represent the geologic contact, which was inclined 8 degrees to the east. Each of these combinations was used to test a different conceptual model for the geologic contact. A two-dimensional model, based on the TRUST computer code, was used, though it was recognized that the flow system was strongly three dimensional in nature. The shaft and inclined geologic contact were simulated in transient mode until steady-state conditions were reached. None of the different conceptual models for the geologic contact produced either a perched water table at the interface or flow into the shaft under steady-state conditions. However, a combination of a welded tuff overlying a nonwelded tuff produced a perched water zone under transient conditions. The saturated zone dissipated as the solution approached steady state. The transient perched water may have occurred because of initial conditions that resulted in additional water moving through the profile.

Fernandez, Hinkebein, and Case (1989) evaluated the impacts of exploratory shafts on performance of the potential Yucca Mountain repository with several different analyses. They concluded that, given the current knowledge of the unsaturated zone hydrology at Yucca Mountain, the presence of the shafts and associated MPZs do not significantly impact the long-term isolation capability of the repository. The

primary concern that they evaluated was the significance of the MPZ on the long-term performance of the potential repository. They performed calculations designed to investigate influx of water to the exploratory shaft by flooding and erosion and by intersection of the shaft by inclined fractures. They determined that flooding events and associated erosion and water flow through fractures contributed a relatively small amount of water to the exploratory shaft, and drainage was expected to be able to handle the amount of water that would result from extreme events. They determined that the presence of the shafts, including the shaft backfill and MPZ, did not significantly affect the performance of the potential repository because of the small amount of water predicted to enter the shaft, even for extreme events.

Fernandez, Hinkebein, and Case (1989) included an evaluation of the impacts of extending the exploratory shafts into the CHn unit. They assumed that extending the shafts into the CHn unit would not reduce the unit to less than its minimum thickness anywhere in the perimeter of the potential repository, based on plans for site characterization at that time. They determined that the impact of water percolating through the shaft backfill and MPZ on the performance of the CHn unit would be negligible because water passing through the exploratory shaft is expected to be separated from wastes stored in the potential repository.

Williams, Vincent, and Bloomsburg (1990) evaluated the impacts of mined openings (drifts) for the potential repository at Yucca Mountain. They used a two-dimensional model, based on the UNSAT2 code, to evaluate the impacts of the drifts on a local flow field in the Topopah Spring welded tuff and to investigate drift design parameters that impact mine water inflow. The design variables they investigated included spacing of drifts, height and width of drifts, and shape of drift roofs. They did not include the effects of the MPZ surrounding mined drifts in their model. They concluded that mine water inflow is possible under conditions of unsaturated flow, and that the rate of mine water inflow is proportional to the magnitude of the recharge. These results are similar to those of Freshley, Dove, and Fernandez (1985), in that a high-recharge rate results in high saturations and that water flow into the drifts was predicted to occur.

Rockhold, Sagar, and Connelly (1990) evaluated unsaturated flow in the vicinity of exploratory shafts at Yucca Mountain. They performed simulations with a three-dimensional model, based on the PORFLO-3© computer code. The three-dimensional model extended from the land surface to the water table, for a total unsaturated zone thickness of 530 m. Two exploratory shafts were represented with a vertical line element feature in the PORFLO-3© code. The exploratory shafts were connected with a short drift located in the Topopah Spring welded unit. The model was used to investigate the influence of the exploratory shafts and MPZs on unsaturated flow through Yucca Mountain. The results demonstrated that the exploratory shafts and MPZs influenced the flow field near the shafts and this influence decreased with depth. Their model results demonstrated that when locally saturated conditions occur, such as near perched water zones, these features may become preferential flow paths. However, they cautioned that

the shafts were treated as one-dimensional features imbedded in three-dimensional computational cells and that the results of the simulations near the shafts are not as accurate as if the features were represented explicitly in the numerical grid. This conclusion influenced the way that the exploratory shaft was treated in our simulations.

1.3 OVERVIEW OF ANALYSIS

The approach to our study was to construct a model of an exploratory shaft (described in Section 2.0), that extends into the CHn unit at Yucca Mountain. The conceptual model is based on the stratigraphy of borehole USW-G4. The numerical model, based on the PORFLO-3© computer code and the conceptual model, is three dimensional, radially symmetric, and centered on an exploratory shaft that extends into the CHn unit to a depth 50 m above the water table. The model builds on past work by Freshley, Dove, and Fernandez (1985); Fernandez, Hinkebein, and Case (1989); and Rockhold, Sagar, and Connelly (1990). Specifically, Rockhold, Sagar, and Connelly (1990) represented shafts in their three-dimensional model with the line element feature in PORFLO-3©. This line element feature is an approximation, and the results predicted with their model are not as accurate as if the feature was explicitly included in the computational grid. Therefore, in this analysis, a smaller region was simulated by restricting the model to the CHn unit and explicitly including the shaft and MPZ in the grid.

The upper boundary condition for the analyses presented in this report was assumed to be uniformly distributed recharge. At depth within Yucca Mountain, the recharge is probably not uniformly distributed because of heterogeneities in the overlying geologic formations. However, the area represented by the upper surface of the radially symmetric model used for these analyses of the shaft extending into the CHn unit is small relative to the surface area of Yucca Mountain. Furthermore, to assume a nonuniform or randomly varying recharge distribution would violate a primary assumption of radial symmetry and would require significantly greater computer resources to address the problem. Therefore, we considered the flux to be uniformly distributed over the upper surface of the model.

The analyses described in this report were completed within a relatively short time (one month). Because of the need to complete the analyses rapidly, existing deterministic models were used. Therefore, this report presents the mean or expected response of the system for the base case and includes perturbations to the mean response introduced by simple variations in the input parameters.

Several different cases were simulated with the radially symmetric model of the shaft to examine the response of the flow system to changes in hydrologic conditions and to compare the total impact of the shaft on the flow regime to undisturbed conditions. Different measures of performance were considered in the analyses. The first performance measure was travel time of the disturbed case compared to the

undisturbed case. The second performance measure was represented by outflow arrival curves that illustrate the distribution of flow at the outflow boundary, in this case the water table, resulting from water flow through the modeled region.

This report is organized as follows: the conceptual model, hydraulic properties, and modeling cases for our study are described in Section 2.0. The simulation results, travel-time comparisons, and outflow arrival curves used to assess the predicted impact of the exploratory shaft extension into the CHn unit are presented in Section 3.0. Conclusions from our study are summarized in Section 4.0, and references cited in this report are contained in Section 5.0.

2.0 MODEL DEVELOPMENT

The objective of this study is to expand on previous investigations of the hydrologic impact of exploratory shafts and drifts at Yucca Mountain to evaluate the impact of extending an exploratory shaft into the CHn unit. This objective requires both estimation of the properties of the MPZ around the shaft and evaluation of the effects of backfill materials and MPZs on travel time. The numerical flow and transport simulator, PORFLO-3© (Runchal and Sagar 1989; Sagar and Runchal 1990) with a particle-tracking algorithm for travel-time calculation, is used to determine the potential effects of shaft backfill materials and MPZs on the travel time of water moving along flow paths from the top of the CHn unit to the water table. The conceptual model, hydraulic properties, initial and boundary conditions used in the numerical model, and specific modeling cases are described in this section.

2.1 CONCEPTUAL MODEL

The conceptual model developed for flow simulations is based on the stratigraphy of borehole USW-G4, as depicted in Figure 2.1. Only the CHn unit is considered in these analyses. This unit is separated into vitric and zeolitic layers based on lithologic characteristics. In the vicinity of borehole USW-G4, the vitric layer is relatively thin (≈5 m), and overlies the thicker (≈125-m) zeolitic layer. In general, both the vitric and zeolitic layers of the CHn unit have few fractures, relative to overlying welded units (Peters et al. 1984). Therefore, no specific fracture effects are considered in the simulations. Data reported in Peters et al. (1984) for two boreholes, USW-G4 and USW-GU3, were assumed to represent the mean physical and hydrologic properties of the CHn unit.

Construction of shafts and drifts in volcanic tuffs and other rocks produces changes in stress fields and in hydrologic properties such as permeability. Case and Kelsall (1987) developed a model of permeability changes as a function of radial distance from a shaft in fractured, welded tuff. Their model was based on analyses that considered modifications in rock mass permeability resulting from stress redistribution and expected increases in fracture frequency within blast-damaged zones caused by shaft excavation. Their model predicts that relative rock mass permeability decreases exponentially with distance from an excavation surface. However, because changes in fracture frequency associated with blasting have not been well documented, their model is regarded as preliminary.

Case and Kelsall (1987) use 1 m as the MPZ dimension in an upper-bound blast-damage model for welded tuff. However, they also note that this dimension actually corresponds to the approximate maximum depth of disturbance measured in dolomite by Worsey (1985) under controlled blasting conditions. Case and Kelsall (1987) speculate that because nonwelded tuff is more ductile than welded tuff, it might

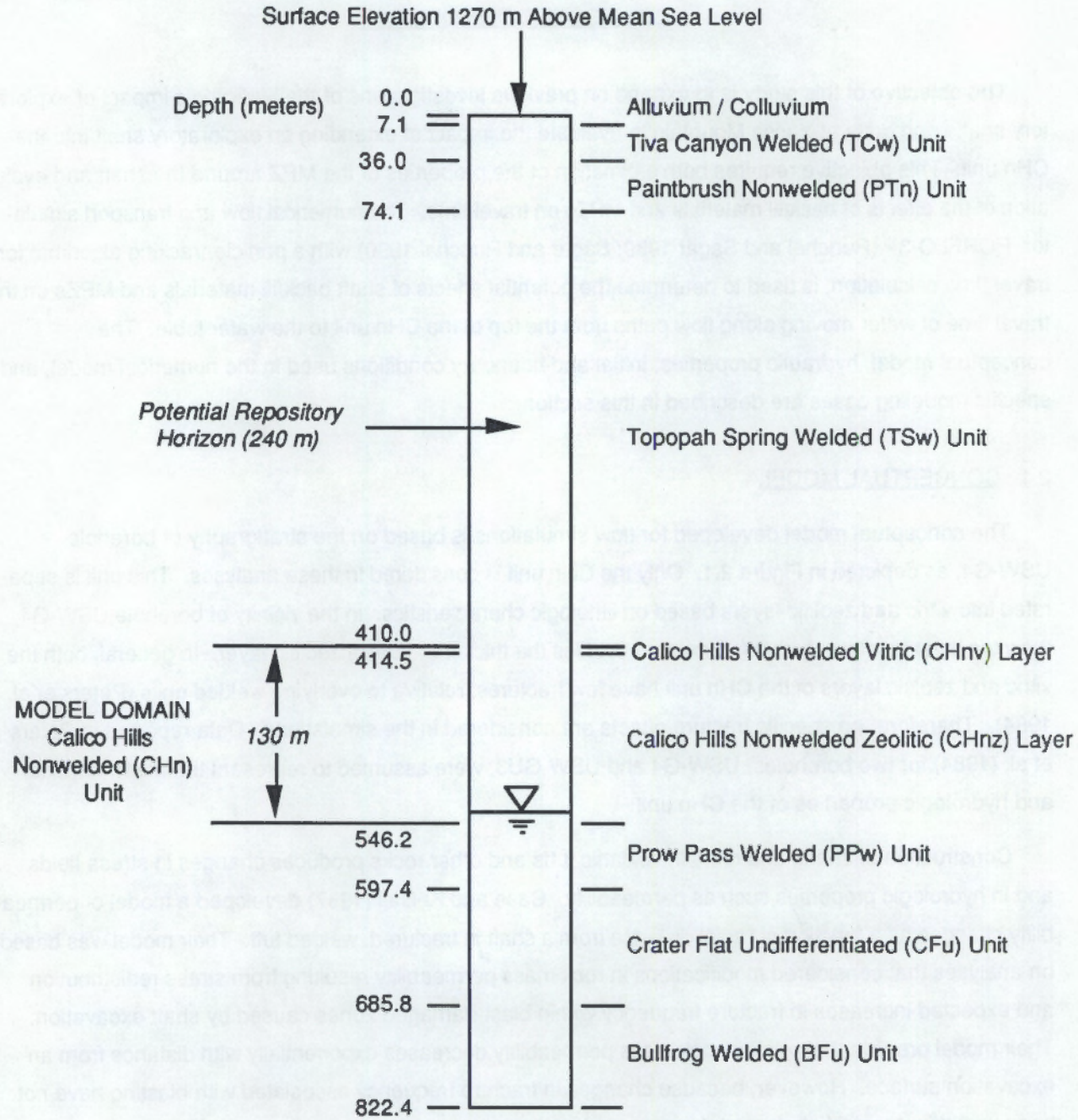

FIGURE 2.1. Generalized Stratigraphy of Borehole USW-G4 (depths from Peters et al. 1984)

sustain greater strain and be less susceptible to fracturing. Therefore, considering that the CHn unit is nonwelded, a 1.0-m MPZ dimension is probably greater than the actual width of the MPZ that would result from excavation of a shaft in this unit.

In our conceptual model, developed for flow simulations and travel-time computations, the exploratory shafts are assumed to be 4.4 m in diameter, with MPZs extending 1.1 m from the shaft walls. Rather than using a function in which relative permeability decreases exponentially with increasing distance from the shaft as described in Case and Kelsall (1987), the entire 1.1-m-wide MPZ is assumed to have a constant permeability. The average properties in this 1.1-m MPZ were derived from the exponential function.

A three-dimensional, radially symmetric model was used for the numerical simulations. Although the volcanic tuffs at Yucca Mountain dip approximately 6 degrees to the east, the effects of tilting beds were assumed negligible for unsaturated flow at the local scale modeled. The exploratory shaft was assumed to extend into the CHn unit to a depth 50 m above the water table. The locations of material zones and the computational grid are depicted in Figure 2.2. Only the inner 10 m of the model are depicted in Figure 2.2, though the computational grid was extended to several model radii, ranging from 10 to 80 m, in our study. After preliminary examination of the effect of maximum radial extent on the solution, the 80-m radius computational grid was employed throughout our study.

2.2 HYDRAULIC PROPERTIES

The vitric layer of the CHn unit is characterized as having a higher saturated hydraulic conductivity and higher porosity than the zeolitic layer (Peters et al. 1984). The van Genuchten (1980) model was used in our study to represent the hydraulic properties of all materials simulated. The model parameters required by the van Genuchten model were the saturated hydraulic conductivity (K_S), the saturated moisture content (θ_S), the residual moisture content (θ_R), and two empirical curve-fitting parameters (α and n). The moisture-retention and hydraulic-conductivity curves for the vitric layers of the CHn unit are shown in Figure 2.3. Figure 2.4 shows the moisture-retention and hydraulic-conductivity curves for the zeolitic layer. Moisture-retention data reported in Peters et al. (1984) are shown as symbols (circles, triangles, and diamonds) in the moisture-retention curves in Figures 2.3 and 2.4. The vertical axis of the moisture-retention curves is the tension head, defined as the negative of the pressure head. The van Genuchten model parameters listed in Figures 2.3 and 2.4 were used in our model simulations.

The hydraulic properties of a gravelly sand (Mualem 1976) were used to represent crushed tuff, the expected backfill material. The moisture-retention and hydraulic-conductivity curves, along with the associated model parameters used to represent this material, are shown in Figure 2.5. Although the selection of these particular properties was arbitrary, we assume that the material to be used for shaft backfill will be coarser and more permeable and will have lower air-entry potentials than the undisturbed CHn unit

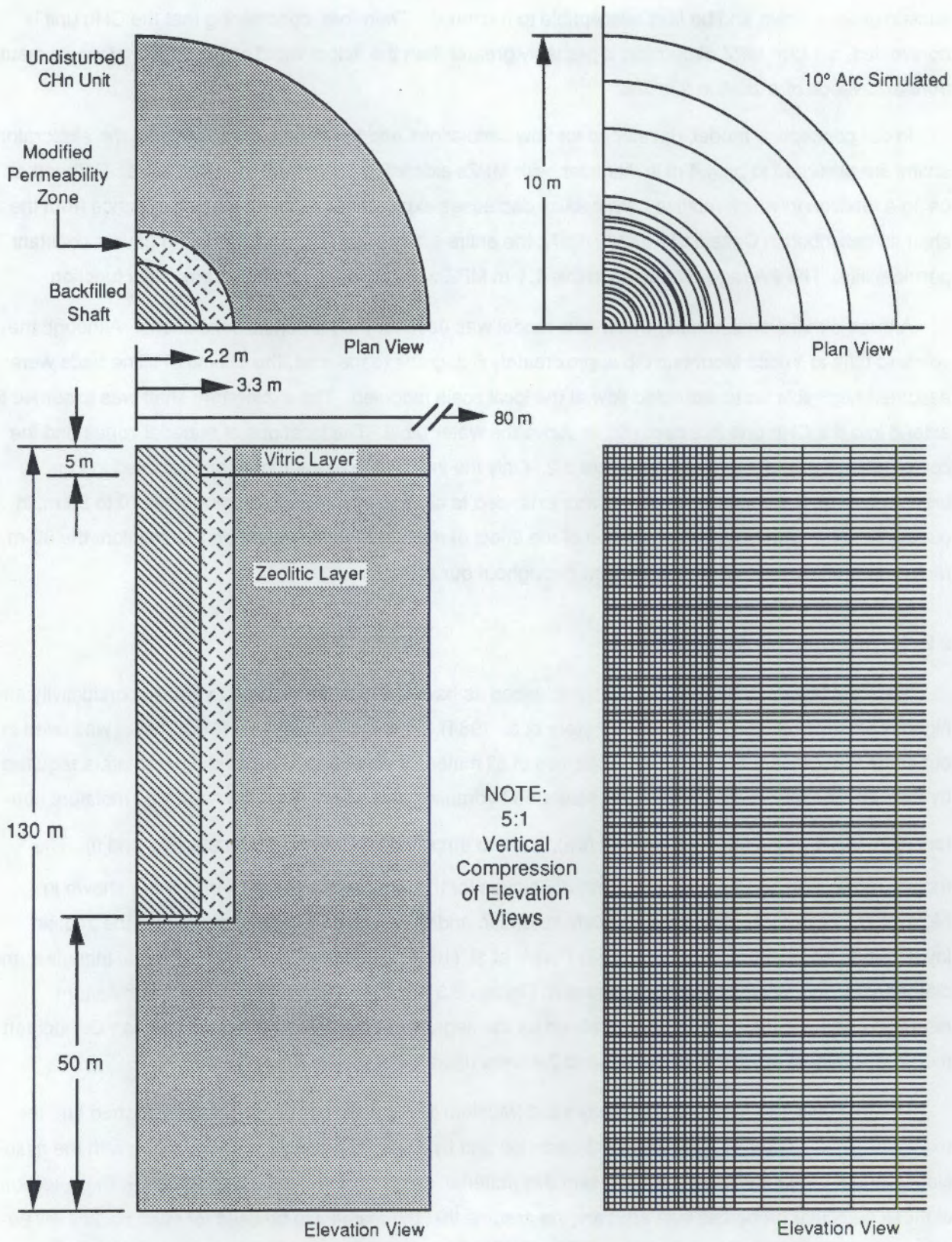

FIGURE 2.2. Material Types and Computational Grid Represented in the Conceptual Model

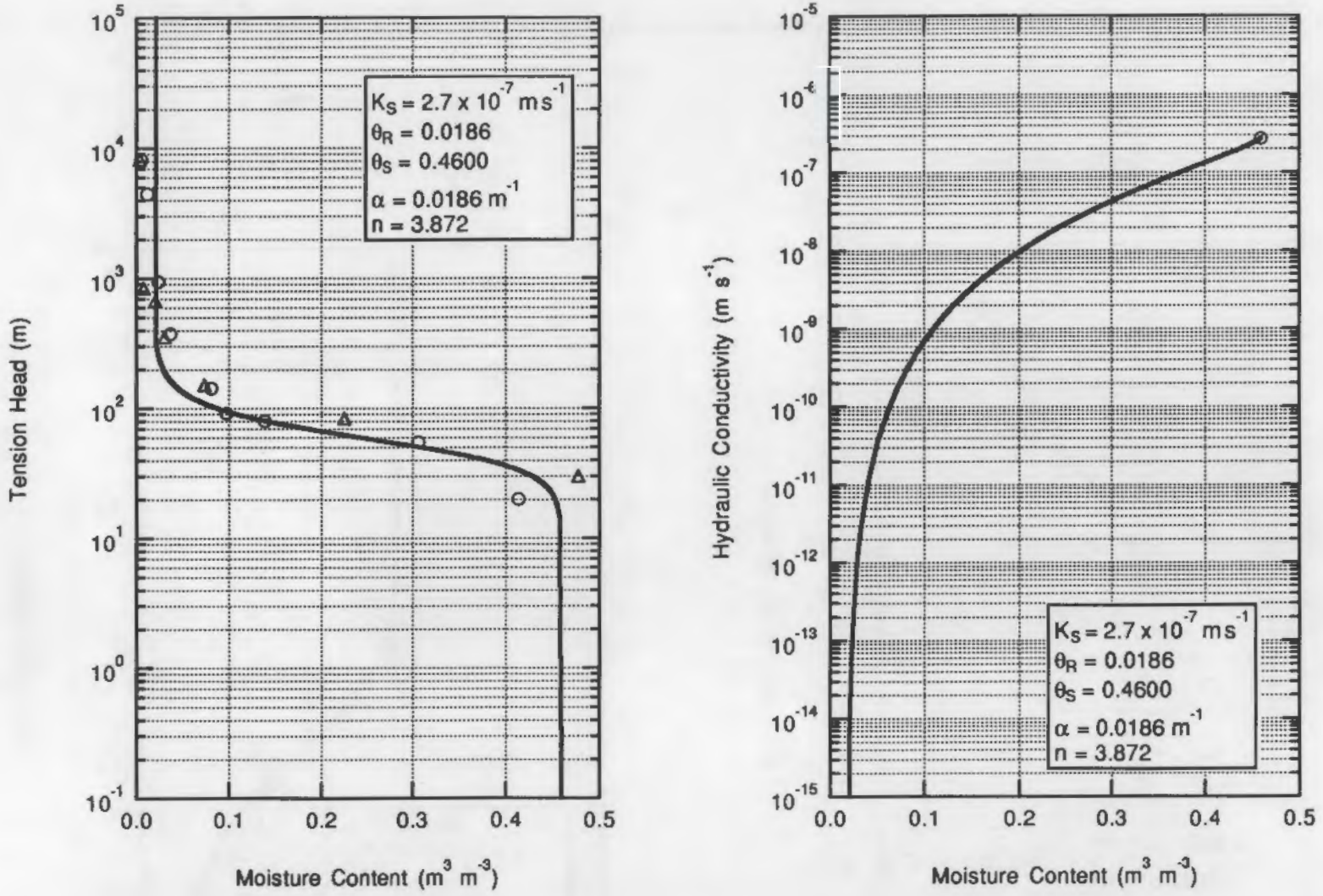

FIGURE 2.3 Moisture-Retention and Hydraulic-Conductivity Curves for Vitric Layer of Calico Hills Nonwelded Unit

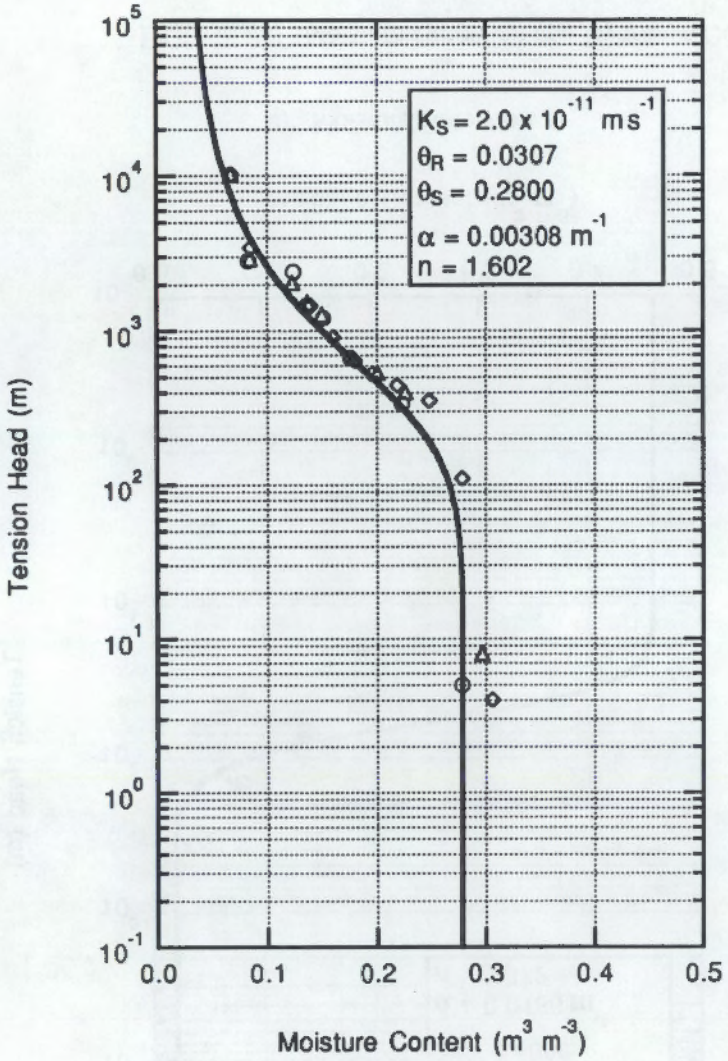

a) Moisture Retention

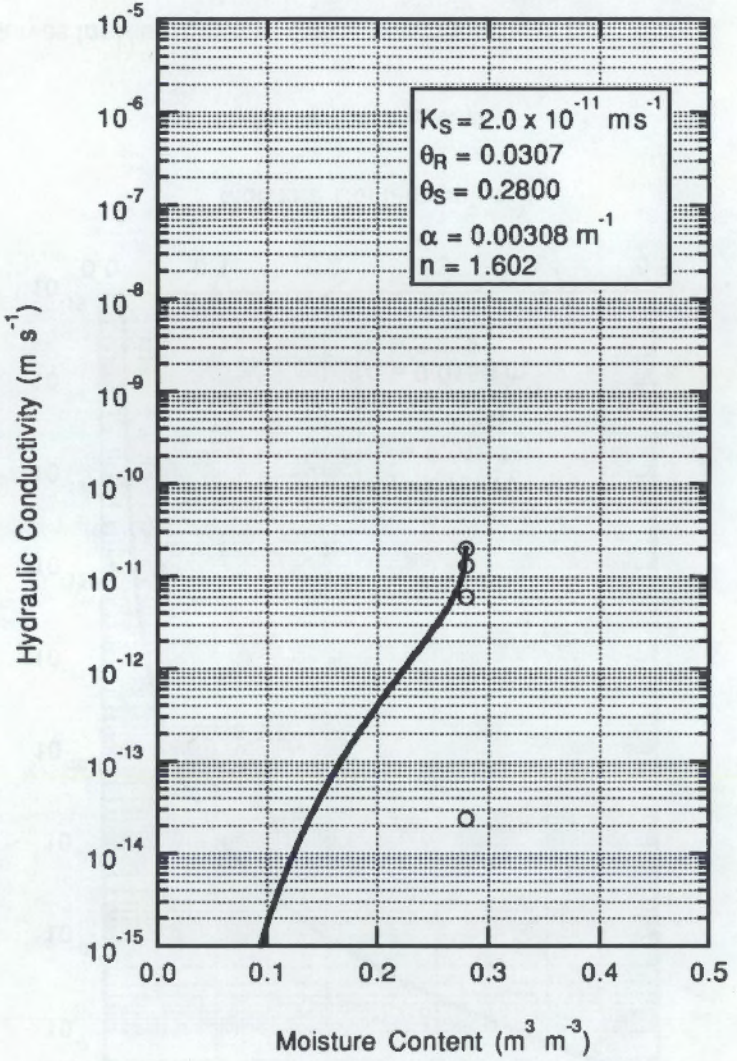

b) Hydraulic Conductivity

FIGURE 2.4 Moisture-Retention and Hydraulic-Conductivity Curves for Zeolitic Layer of Calico Hills Nonwelded Unit

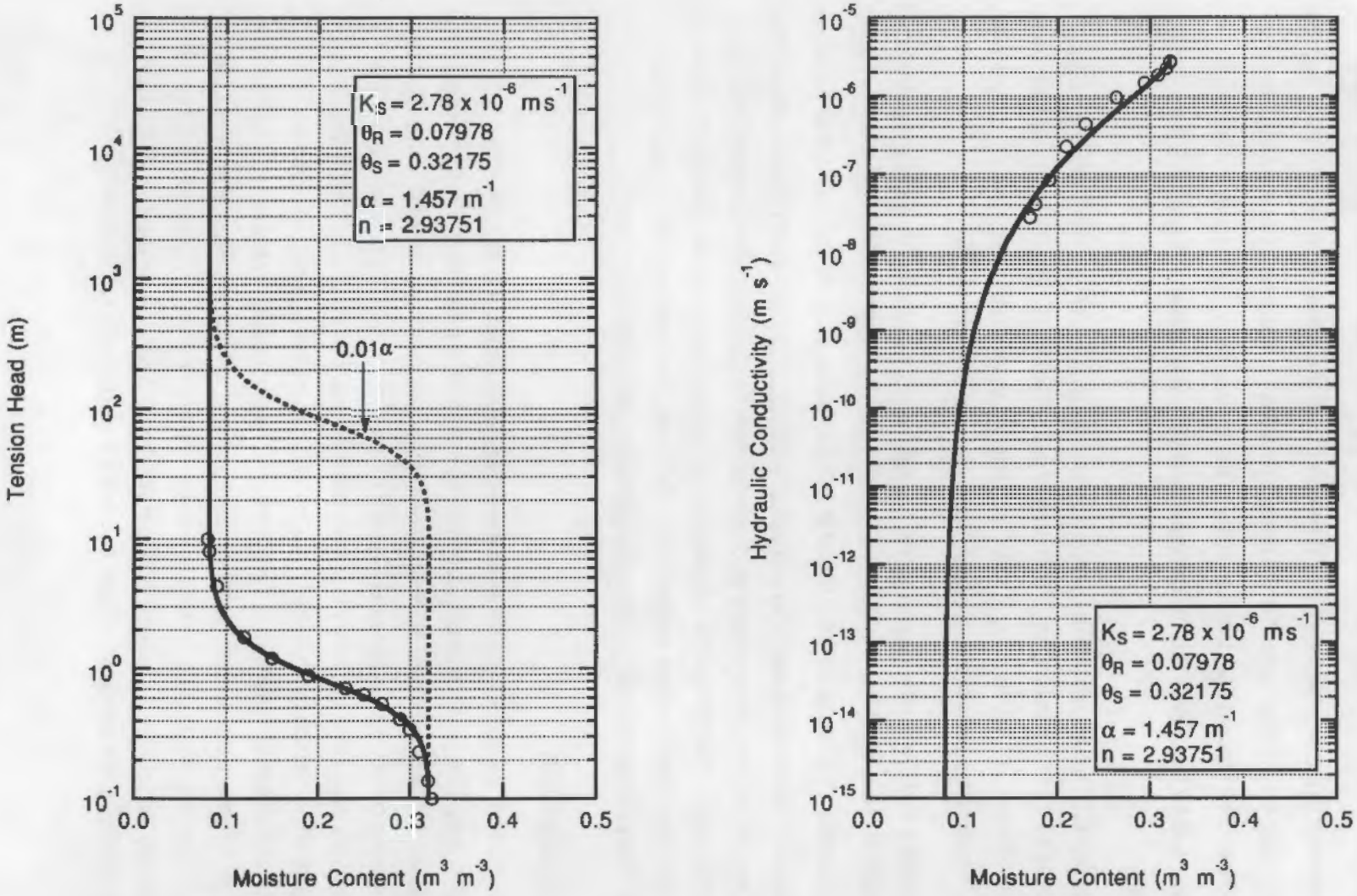

FIGURE 2.5 Moisture-Retention and Hydraulic-Conductivity Curves for 4135 Gravelly Sand (Mualem 1976)

(Freshley, Dove, and Fernandez 1985). One case (described in Section 2.4) was developed to demonstrate the importance of the α curve-fitting parameter by using a value 0.01 times the expected value. Because α is the inverse of the air-entry head, this increases the air-entry head by a factor of 100. Implicit in a higher air-entry head for the shaft backfill is the greater potential for water flow into the shaft from the surrounding formation. The dashed line, labeled 0.01α in the moisture-retention curve in Figure 2.5, shows the appropriate fit for this case. The hydraulic-conductivity curve shown in Figure 2.6 is the same for the 0.01α case.

Case and Kelsall (1987) estimated that the average permeability of the MPZs in the Topopah Spring welded tuff unit could be 20 to 80 times greater than that of the undisturbed rock. These estimates were made for depths of 100 and 310 m below the surface, considering overburden stress and the variation in hydraulic and mechanical properties in the Topopah Spring welded unit with depth.

For flow simulations and travel-time computations, the saturated hydraulic-conductivity value assigned to the MPZs in the CHn unit is assumed to be 20 times greater than that of the undisturbed rock. In addition, the air-entry potential ($1/\alpha$) of the MPZs in the CHn unit was assumed to be one-half that of the undisturbed rock. Selection of these values was also somewhat arbitrary, but again reflects the assumption that the MPZs in the CHn unit will effectively behave as coarser porous media with higher permeabilities relative to the undisturbed rock. The CHn unit is nonwelded, and is assumed to be less disrupted by construction of the exploratory shaft than are welded units. Therefore, the lower degree of disruption or factor of increased hydraulic conductivity (20) is employed for the MPZ in the CHn unit.

2.3 BOUNDARY CONDITIONS

The elevation datum for the model was taken as the water table, assumed to coincide with the lower boundary of the CHn unit. The lower boundary condition is, therefore, a prescribed-pressure boundary at atmospheric pressure. A one-dimensional model of the CHn unit, without shafts or MPZs, was used to provide a pressure-head distribution (depicted in Figure 2.6) and undisturbed travel-time value. The outer boundary opposite the axis of symmetry is a prescribed-pressure boundary, or Dirichlet condition, equal to the pressure-head distribution obtained from the one-dimensional, undisturbed model. The boundary along the shaft's axis of symmetry is a prescribed no-flow boundary, or Neumann condition, for all cases. The upper boundary is a uniform, constant-flux boundary, or Neumann condition, with a value of 0.1 or 0.3 mm yr^{-1}. The assumption of a uniform flux across the upper boundary presupposes that the flux is not influenced by the overlying Topopah Spring welded unit. Variations in the specified boundary conditions will be discussed in a subsequent description of the modeling cases (Section 2.4).

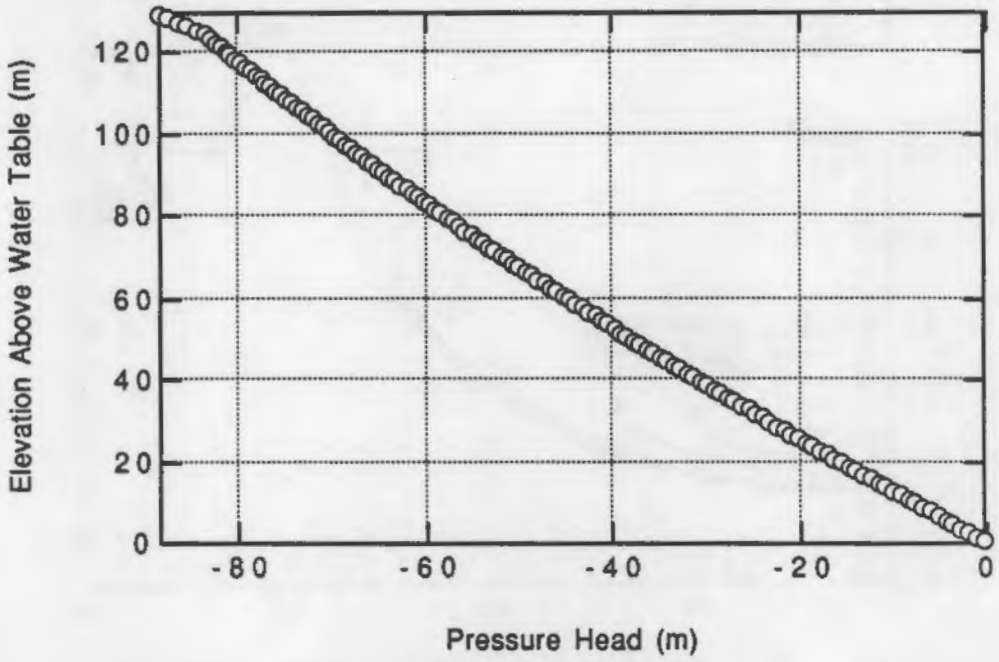

FIGURE 2.6. Pressure-Head Profile from One-Dimensional Model Simulation

Preliminary simulations with the radial model were conducted using successively larger model radii to ensure that the radial dimension of the model domain was large enough to minimize the effects of the outer boundary on the solution near the shaft. To evaluate the adequacy of different model radii, a particle-tracking algorithm was used and travel time was plotted as a function of radial distance from the model's axis of symmetry. The 0.01α condition was used to size the model with this method because this condition allows more water to enter the shaft, and hence, leads to a larger radius of influence by the shaft. Figure 2.7 shows travel time as a function of initial radial distance of travel-time particles for a number of different model radii. When the travel time reached the undisturbed, steady-state travel time and remained at that value with increasing radial distance, the model radius was assumed to be sufficiently large. It was determined that a radial dimension of approximately 80 m was required to minimize the effects of the outer boundary on the solution near the shaft. This is demonstrated by the nearly identical traces in Figure 2.7 for the 70- and 80-m model radii. In contrast to the 0.01α condition, use of the expected value of α leads to quite different results, as shown in Figure 2.8. The smaller radius of influence (in Figure 2.8) indicates that the 80-m-radius model is more than adequate to minimize the effects of the outer boundary on the solution near the shaft.

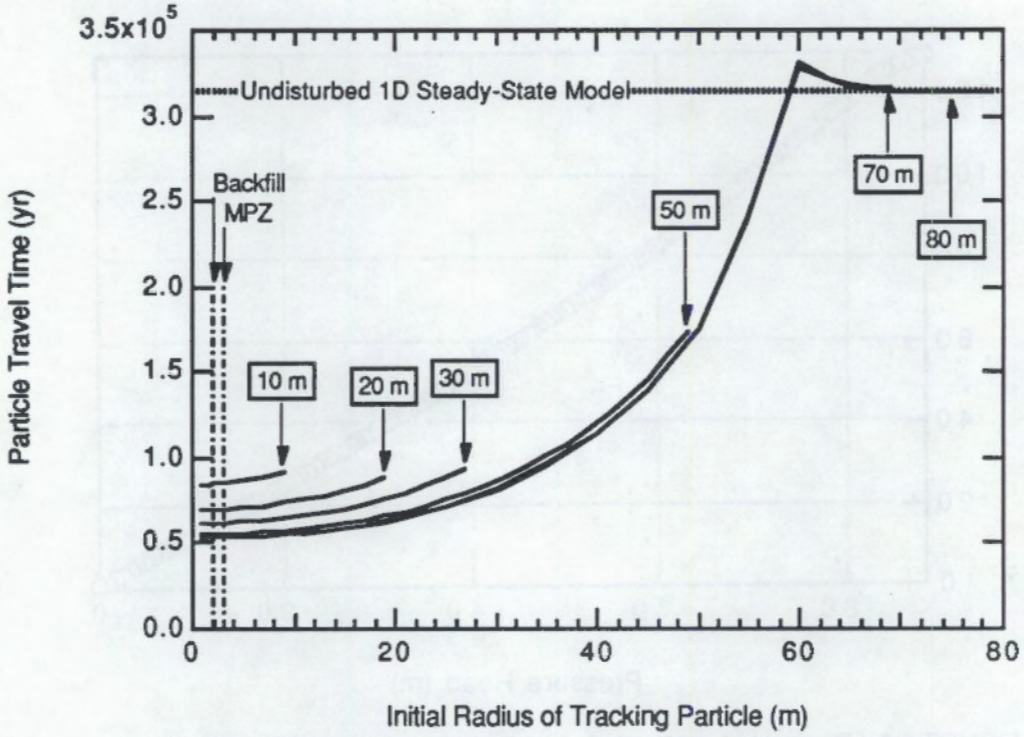

FIGURE 2.7. Travel Time as a Function of Radial Distance for Different Model Radii and $\alpha = 0.01457\ m^{-1}$

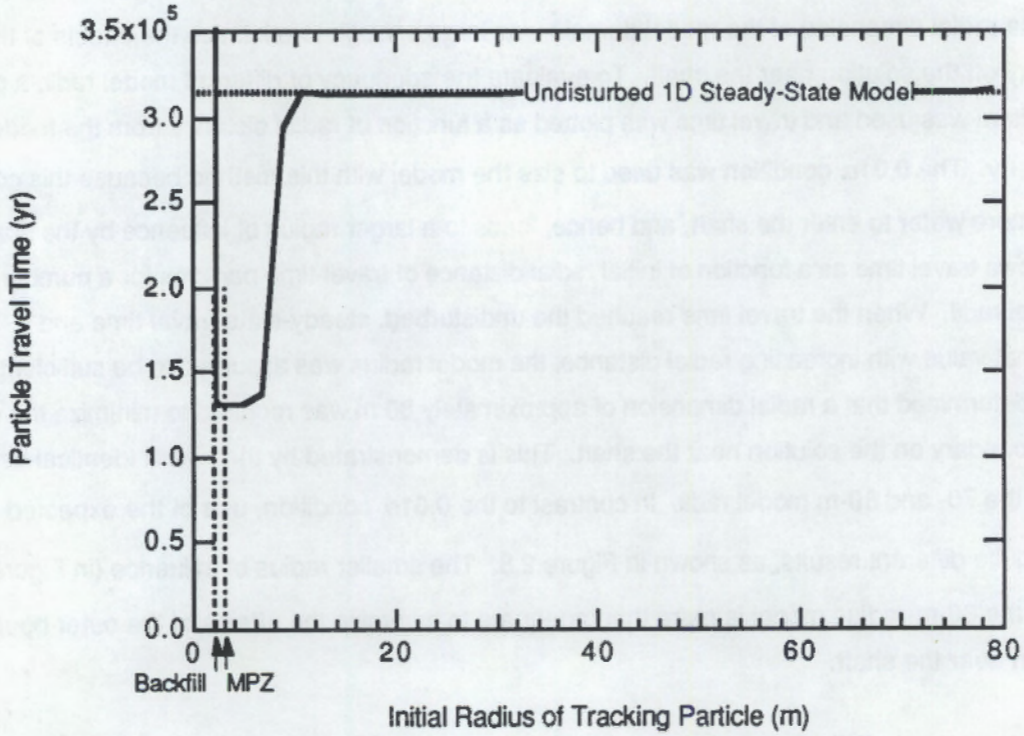

FIGURE 2.8. Travel Time as a Function of Radial Distance for Different Model Radii and $\alpha = 1.457\ m^{-1}$

2.4 MODELING CASES

The average annual precipitation at Yucca Mountain is estimated to be approximately 150 mm yr^{-1} (Montazer and Wilson 1984). An upper-bound estimate of recharge to the saturated zone is approximately 0.50 mm yr^{-1} (Montazer and Wilson 1984). However, the downward flux in the CHn unit is estimated to be limited to approximately 0.006 mm yr^{-1} (Montazer and Wilson 1984). Several modeling cases were simulated to determine the response of the flow field in the vicinity of the extended shaft, the effects of different recharge rates, the effects of the vitric layer of the CHn unit, the potential for formation of perched water zones, and the results of shaft flooding.

The base case represents the expected hydrologic conditions in the CHn unit based on available data. Two versions of the base case are simulated to provide hydrologic conditions for the undisturbed flow field (i.e., without the shaft or MPZs) and for the disturbed flow field after extension of an exploratory shaft into the CHn unit. The undisturbed flow field is simulated with a one-dimensional model and a recharge flux of 0.1 mm yr^{-1}. The steady-state pressure distribution obtained from this simulation is used to specify the initial and outer boundary conditions for the disturbed two-dimensional flow field simulation.

Potentially adverse conditions of the site were examined by extension of the base case. The high-recharge case is identical to the base case, except that the recharge flux is increased to 0.3 mm yr^{-1}. The high-recharge case is designed to explore the impact of underestimating the recharge rate through the CHn unit on predicted performance. The no-vitric case is defined by the reduction of the model to include only the zeolitic layer of the CHn unit. This case is designed to illustrate the importance of the vitric layer by comparison of a simulation without that layer to other cases with it. The thin-perching-layer case is a revision of the model in which a hypothetical, thin, low-permeability zone is embedded in the model domain at an elevation of approximately 85 m above the water table. This case was included to determine the potential for perched water to occur over a zone of lower permeability. The importance of the value of the curve-fitting parameter α, the inverse of the air-entry potential of the shaft backfill material, is demonstrated in the low-alpha case. The low-alpha case is identical to the base case, except that the value of α for the shaft backfill is divided by 100. The final case is the shaft-water-release case, representing a flooding scenario in which the recharge rate into the top of the shaft is very high (equal to one-half the saturated hydraulic conductivity of the backfill). The 0.01α condition is also used in this case. This case is the least realistic because it is based on introduction of water on a scale not expected at Yucca Mountain and because it ignores the use of shaft seal materials in the overlying Topopah Spring welded unit that would prevent such an event. This final case was included to examine the response of the disturbed CHn unit to a large water flow down the shaft, however unlikely the event.

3.0 MODEL RESULTS

3.1 SIMULATION RESULTS

Simulations of the radially symmetric shaft model (described in Section 2.0) are presented in this section. The design and rationale for each case were presented in Section 2.4.

3.1.1 Base Case

Figure 3.1 depicts the hydraulic-head contours simulated for the base case in the RZ plane. The hydraulic heads range from 0 m at the water table to greater than 41 m at the upper boundary. The R dimension (horizontal axis) of Figure 3.1 is the radial distance, ranging from 0 m at the center of the backfilled shaft to 80 m at the outer boundary. The hydraulic-head contour lines are nearly horizontal throughout the model domain, indicating that the influence of the shaft and MPZ on the flow regime is minimal for expected conditions. The saturation contours for the base case are shown in Figure 3.2. The range of saturations within the zeolitic layer is small, from 0.95 to 1.0. The large contrast in saturation is at the boundary between the vitric and zeolitic layer and within the shaft. Streamlines, the paths that water particles take in the porous media under steady-state conditions, are shown for the base case in Figure 3.3. These paths correspond to the 30 particles used to compute the travel times shown in Figure 2.7. The deflection of streamlines from vertical paths point out that the vitric layer is more influenced by the shaft than the zeolitic layer and, owing to its higher hydraulic conductivity, the relatively high-saturation level, and the interface between the vitric and zeolitic layers, the MPZ appears to act as a vertical preferential flow path.

3.1.2 High-Recharge Case

The high-recharge case was identical to the base case, except that the constant flux at the upper boundary was changed from 0.1 to 0.3 mm yr^{-1}. The hydraulic-head contours for this model, shown in Figure 3.4, range from 0 m at the water table to greater than 88 m at the upper boundary. This range is over twice that of the base case. As with the base case, the hydraulic-head contour lines are nearly horizontal throughout the model domain. The saturation contours in Figure 3.5 indicate that the range of saturations in the zeolitic layer is still narrow (0.95 to 1.0), but in this case, the vitric layer is also nearly saturated (approximately 0.90). Travel time is shorter throughout the model domain because the recharge is higher and saturations are not significantly higher. Streamlines for the high-recharge case are shown in Figure 3.6. Unlike the base case, these streamlines are not essentially vertical in the vitric layer. At higher saturations, the vitric layer begins to function as a horizontal preferential flow path and directs water toward the MPZ. The combined effect of the high-conductivity vitric layer and the MPZ is to decrease travel time in the vicinity of the shaft. Therefore, the high-conductivity vitric layer is important at higher recharge rates.

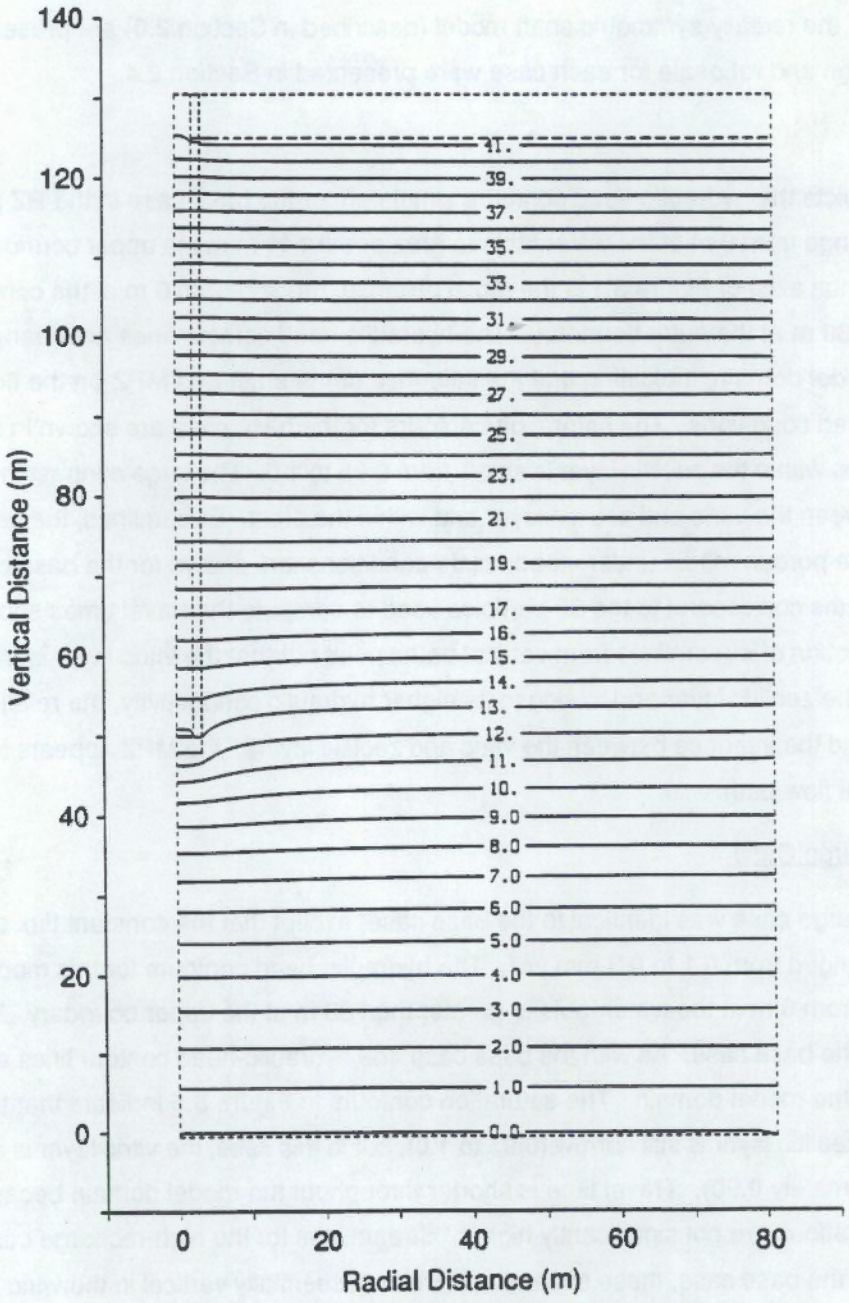

FIGURE 3.1. Hydraulic-Head Contours for Steady-State Solution of Base Case

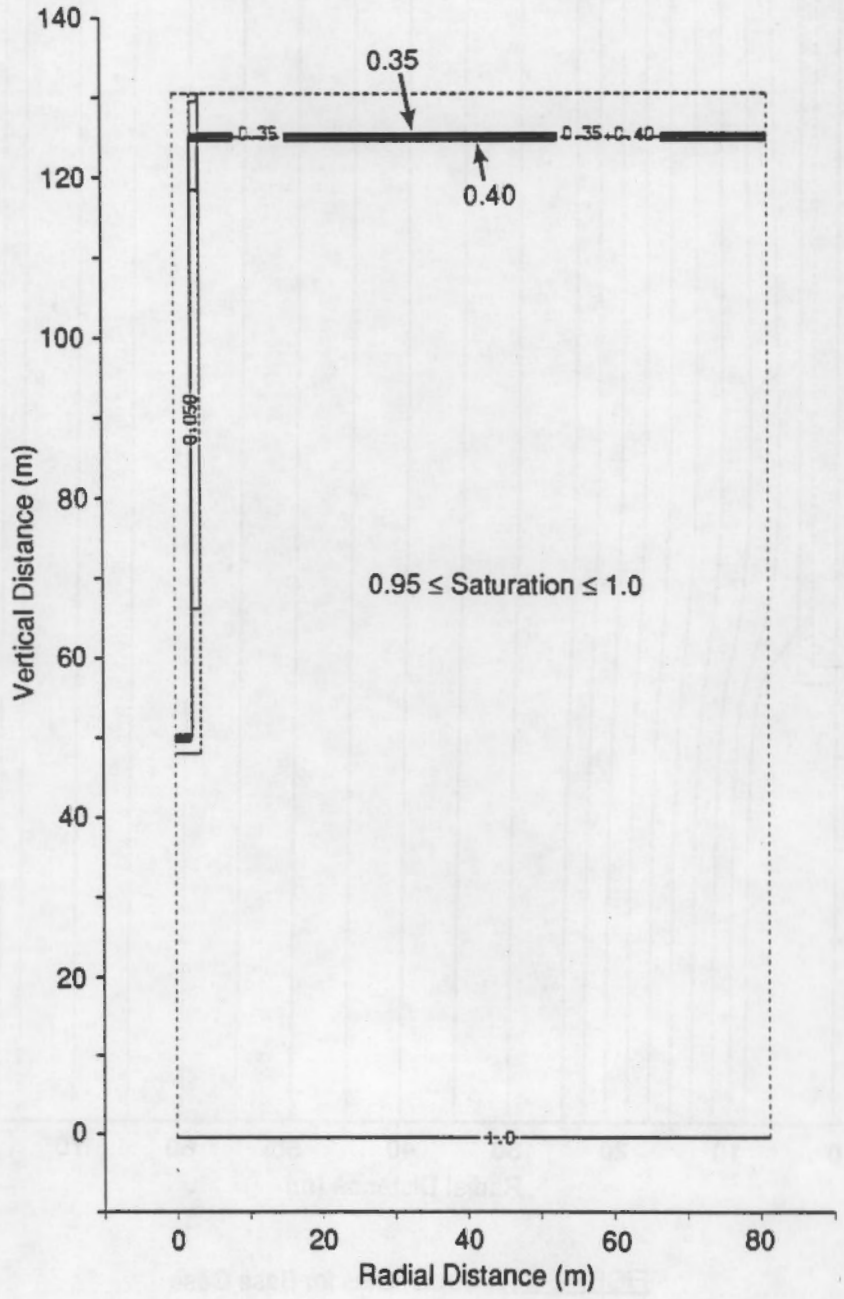

FIGURE 3.2. Saturation Contours for Steady-State Solution of Base Case

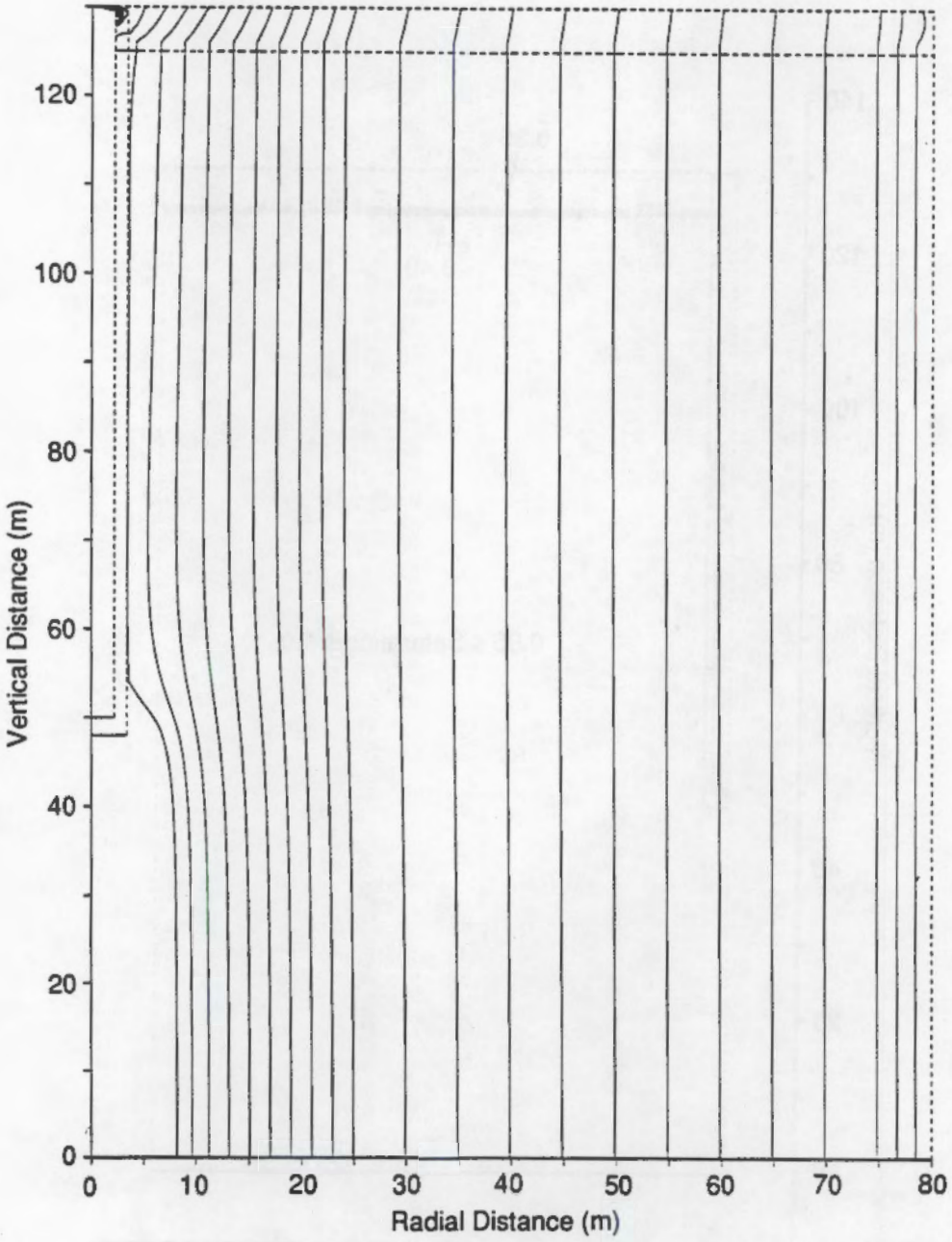

FIGURE 3.3. Streamlines for Base Case

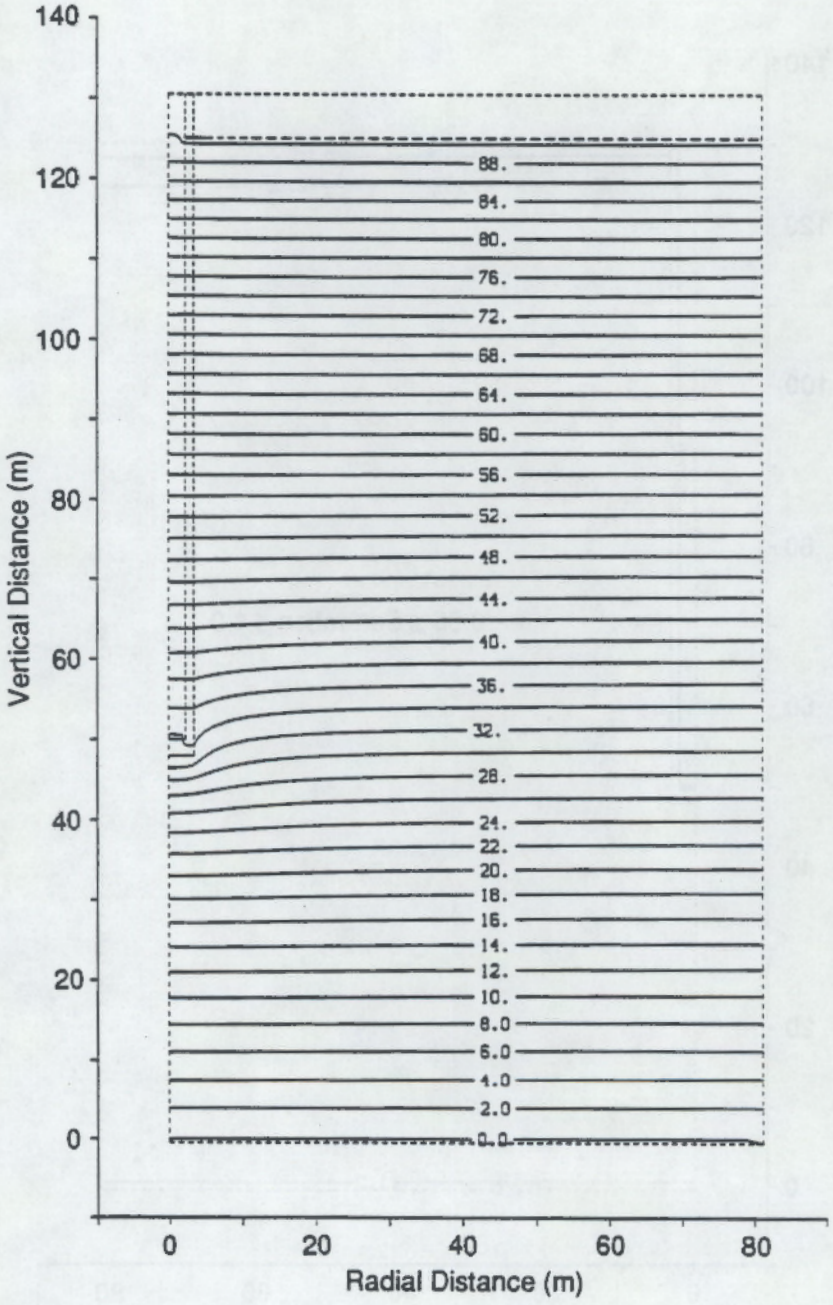

FIGURE 3.4. Hydraulic-Head Contours for Steady-State Solution of High-Recharge Case

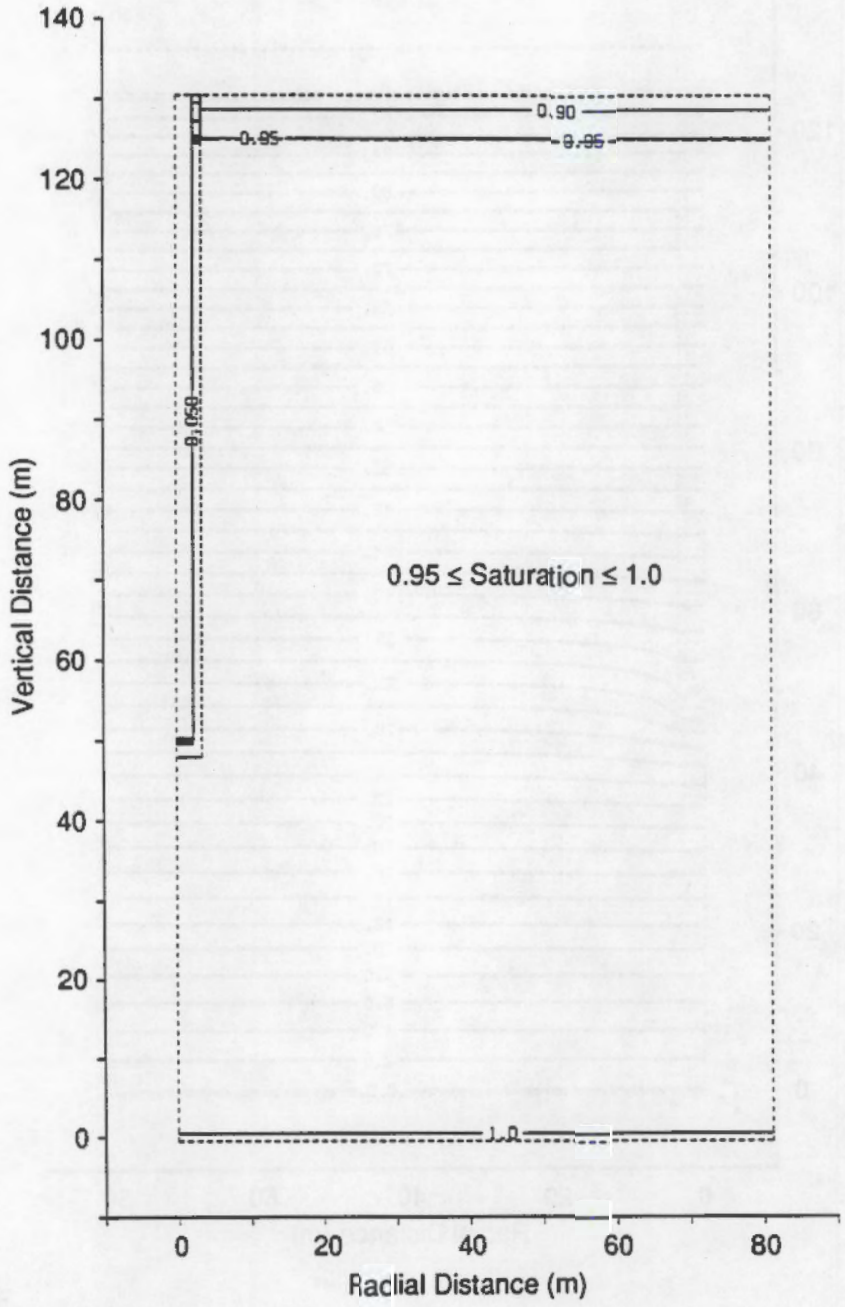

FIGURE 3.5. Saturation Contours for Steady-State Solution of High-Recharge Case

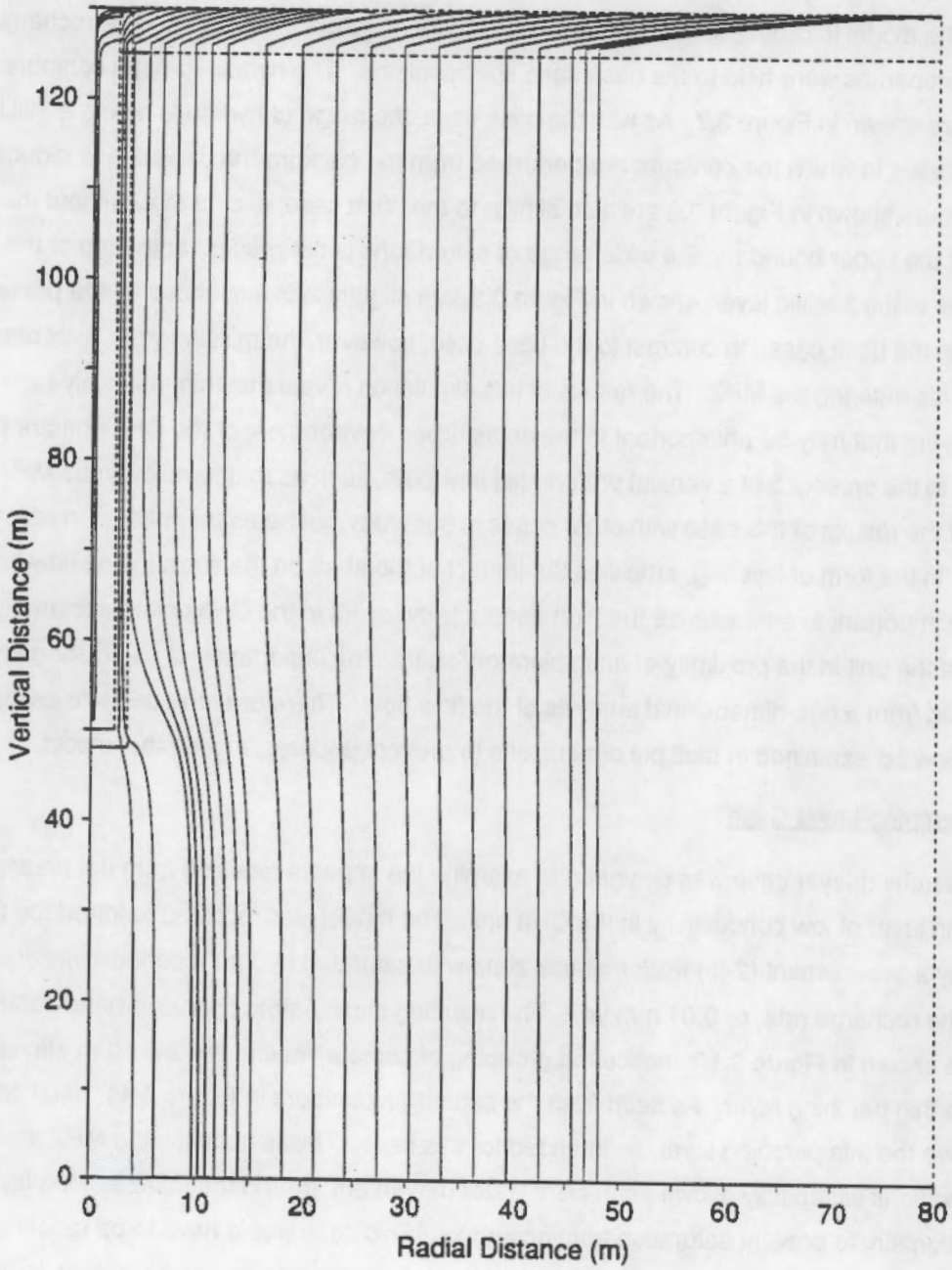

FIGURE 3.6. Streamlines for High-Recharge Case

3.1.3 No-Vitric Case

The base case was modified by removing the vitric layer to demonstrate the importance of the heterogeneity introduced by the contrast between the vitric and zeolitic layers through comparison with other cases. The model thickness for the no-vitric case is 125 m, rather than 130 m. The recharge rate and hydraulic properties were held to the base case specifications. The hydraulic-head contours for the no-vitric case are shown in Figure 3.7. As with the base case, the range of hydraulic heads is still from 0 to 41 m, but the radius in which the contours are perturbed from the background condition is reduced. The saturation contours shown in Figure 3.8 are also similar to the base case, except that, without the contrast in properties at the upper boundary, the wide range of saturations is not present at the top of the model. The streamlines in the zeolitic layer, shown in Figure 3.9, are slightly less influenced by the presence of the shaft than in the base case. In contrast to the base case, however, the missing vitric layer results in fewer streamlines entering the MPZ. The results of this simulation reveal that thin, relatively high-conductivity layers that may be unimportant in the undisturbed environment of the CHn unit are potentially very important in the presence of a vertical preferential flow path, such as that formed by the MPZ. Comparison of the results of this case with other cases in our study illustrates the manner in which heterogeneity, in the form of layering, amplifies the impact of the shaft on the surrounding flow field. It is, therefore, very important to characterize the high-conductivity layers in the CHn unit to accurately predict performance of the unit in the proximity of an exploratory shaft. The importance of contrasting layers could not be observed from a one-dimensional analysis of the flow field. Therefore, an adequate assessment requires that flow be examined in multiple dimensions to prevent underestimating the impact.

3.1.4 Thin-Perching-Layer Case

The thin-perching-layer case was designed to examine the impacts resulting from the presence of an undetected thin layer of low conductivity in the CHn unit. The model was modified to introduce this layer, represented by a two-element (2-m) thick material zone with saturated hydraulic conductivity equal to one-tenth of the recharge rate, or 0.01 mm yr^{-1}. The resulting steady-state hydraulic-head contours for this model are shown in Figure 3.10: notice the grouping of contour lines at the Z = 80-m elevation, the location of the thin perching layer. As seen from the saturation contours in Figure 3.11, perched water did not occur above the thin perching layer, as intended for this case. This is because the MPZ and outer boundary conditions essentially allowed sufficient water movement around the thin perching layer, or out of the model domain, to prevent saturation from occurring. This case would have to be redefined so that the outer boundary represented a no-flow boundary, or approximated an infinite boundary, to force perched water to occur in the upper portion of the zeolitic layer. We expect that, under such modeling constraints, the perching layer would be shown to be more important than was demonstrated in this case. Streamlines for the thin-perching-layer case are shown in Figure 3.12: notice the vertical path that the streamlines follow through the thin perching layer.

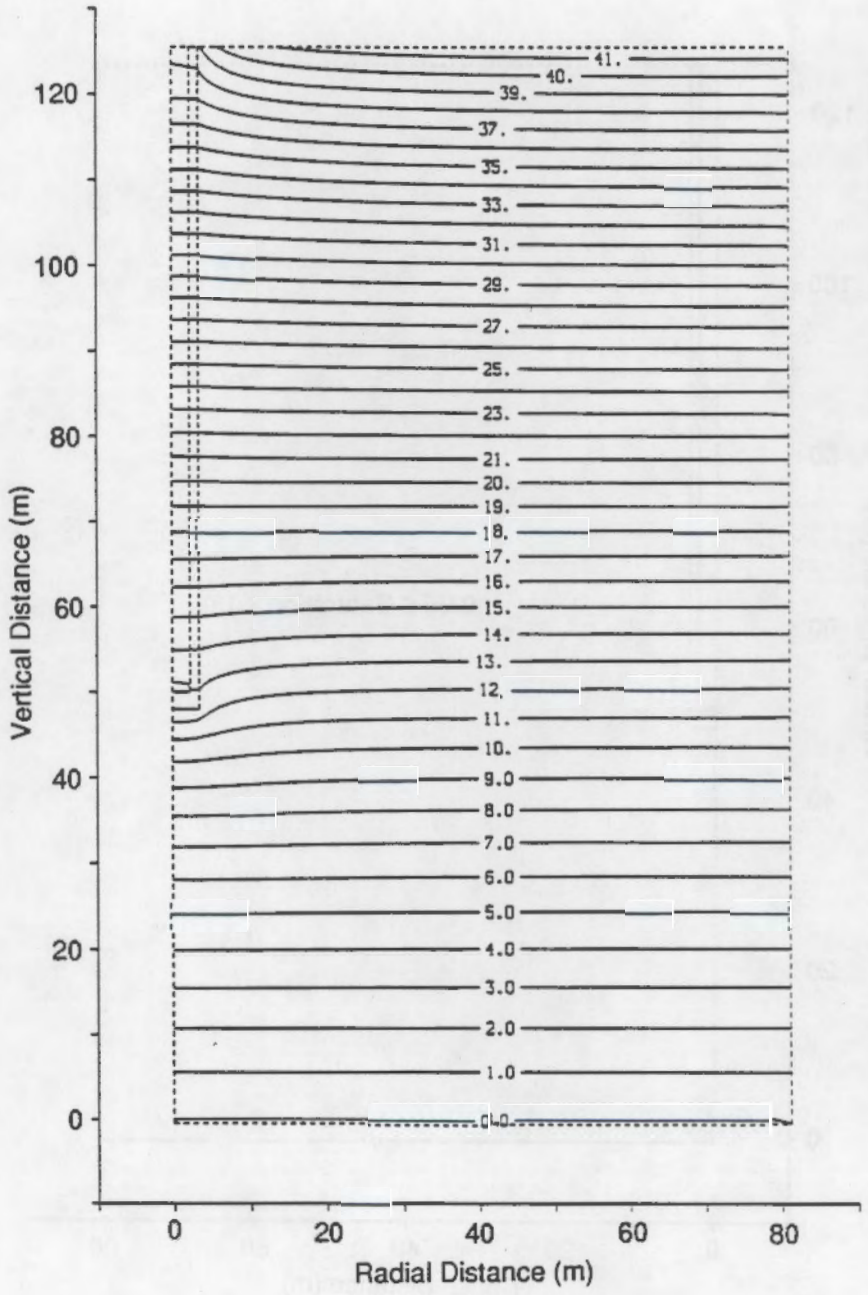

FIGURE 3.7. Hydraulic-Head Contours for Steady-State Solution of No-Vitric Case

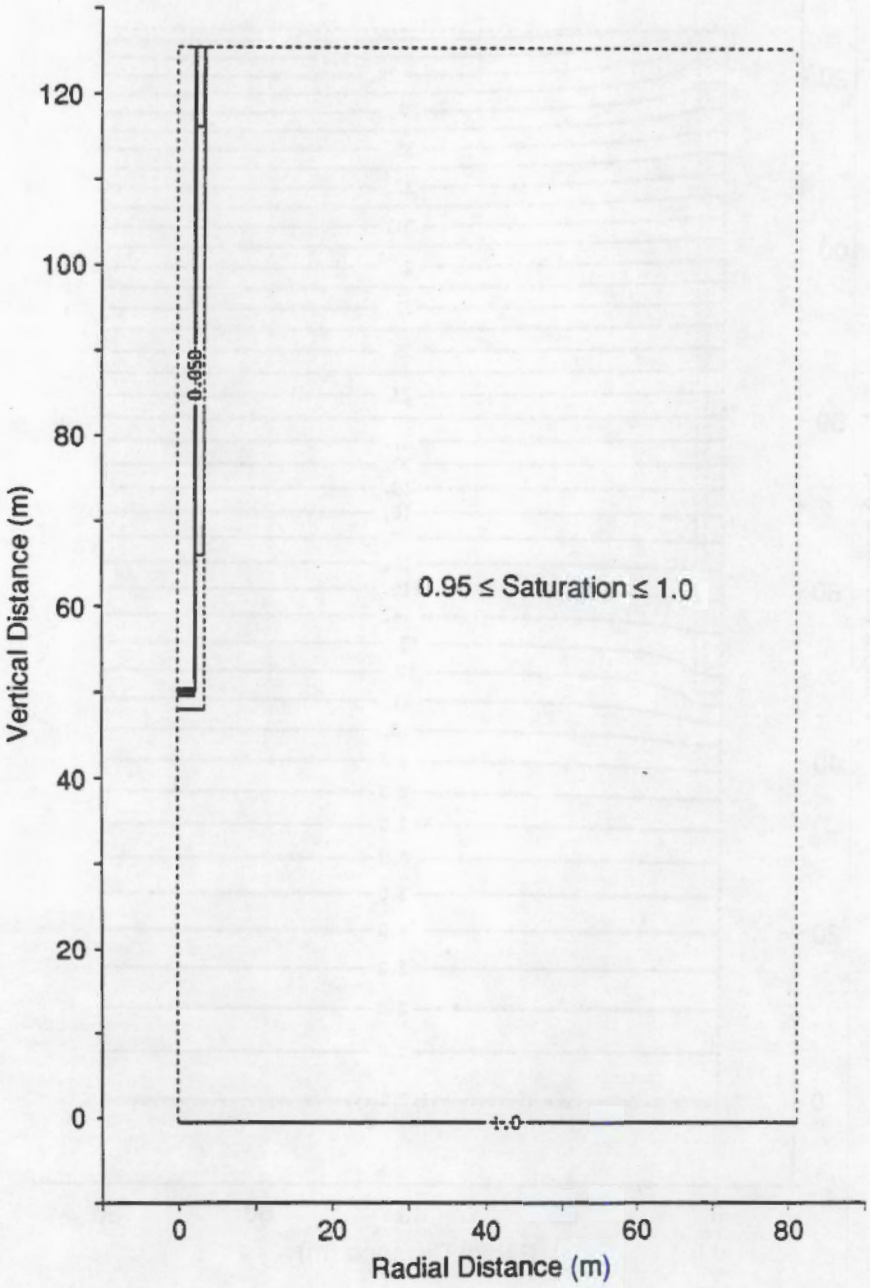

FIGURE 3.8. Saturation Contours for Steady-State Solution of No-Vitric Case

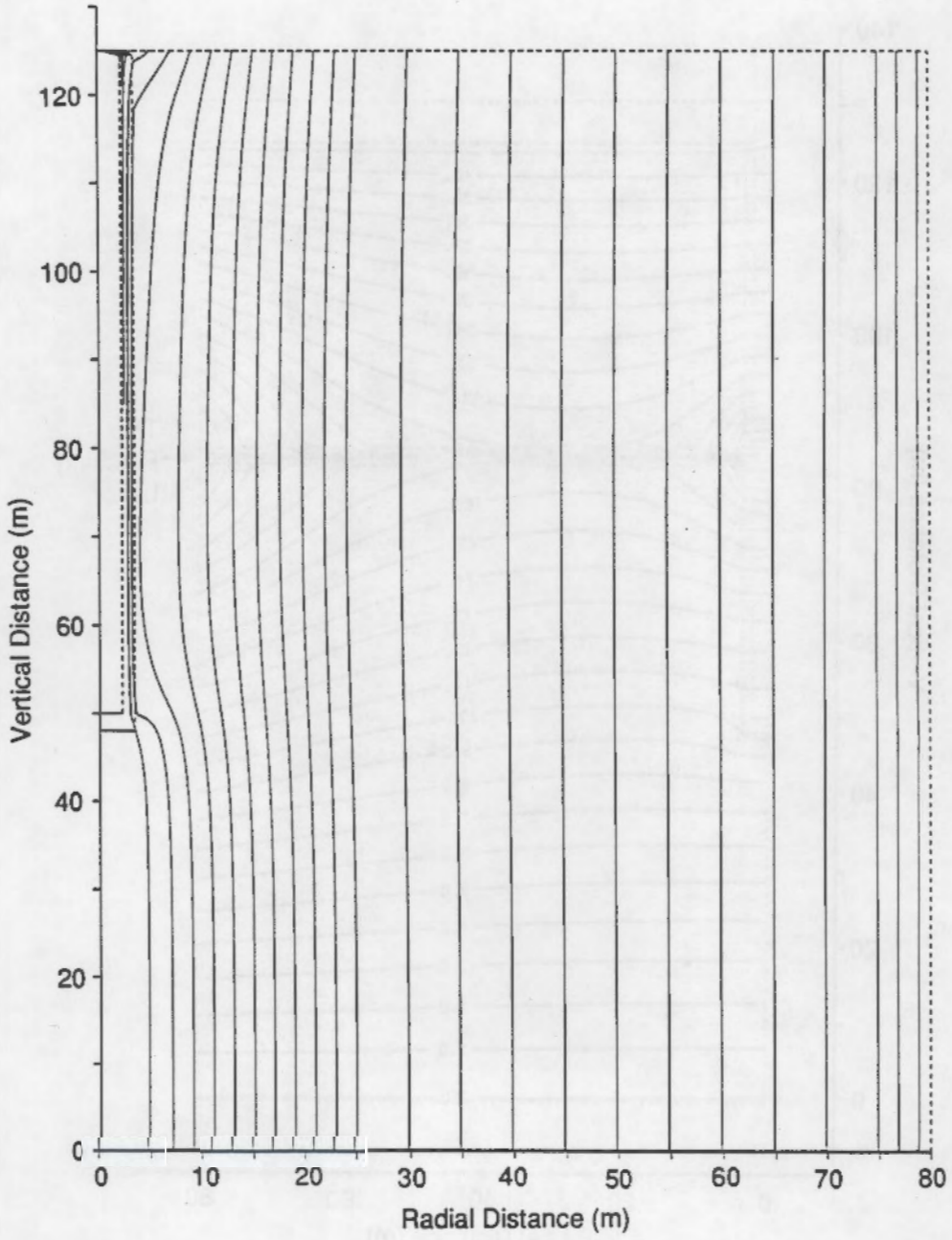

FIGURE 3.9. Streamlines for No-Vitric Case

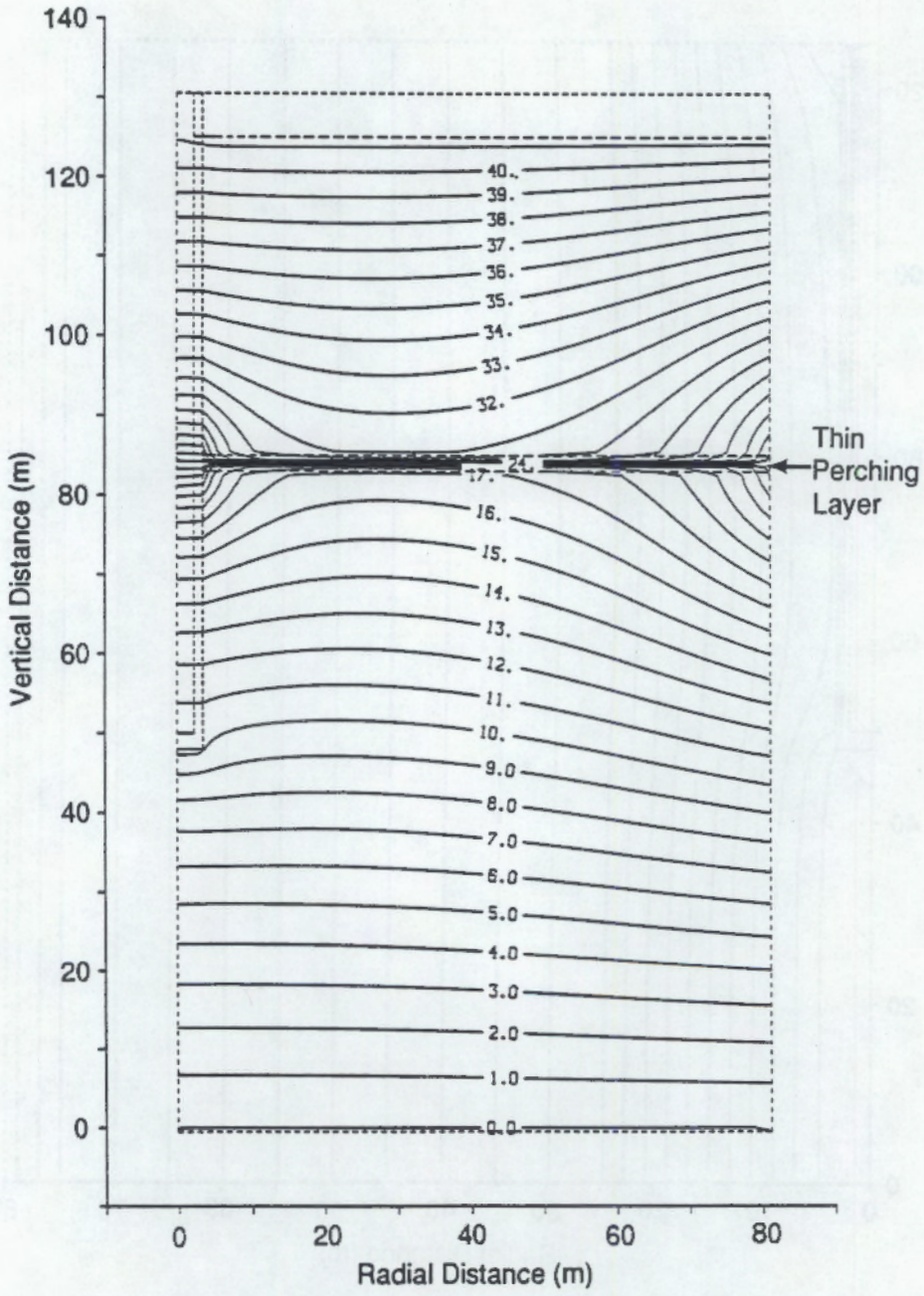

FIGURE 3.10. Hydraulic-Head Contours for Steady-State Solution of Thin-Perching-Layer Case

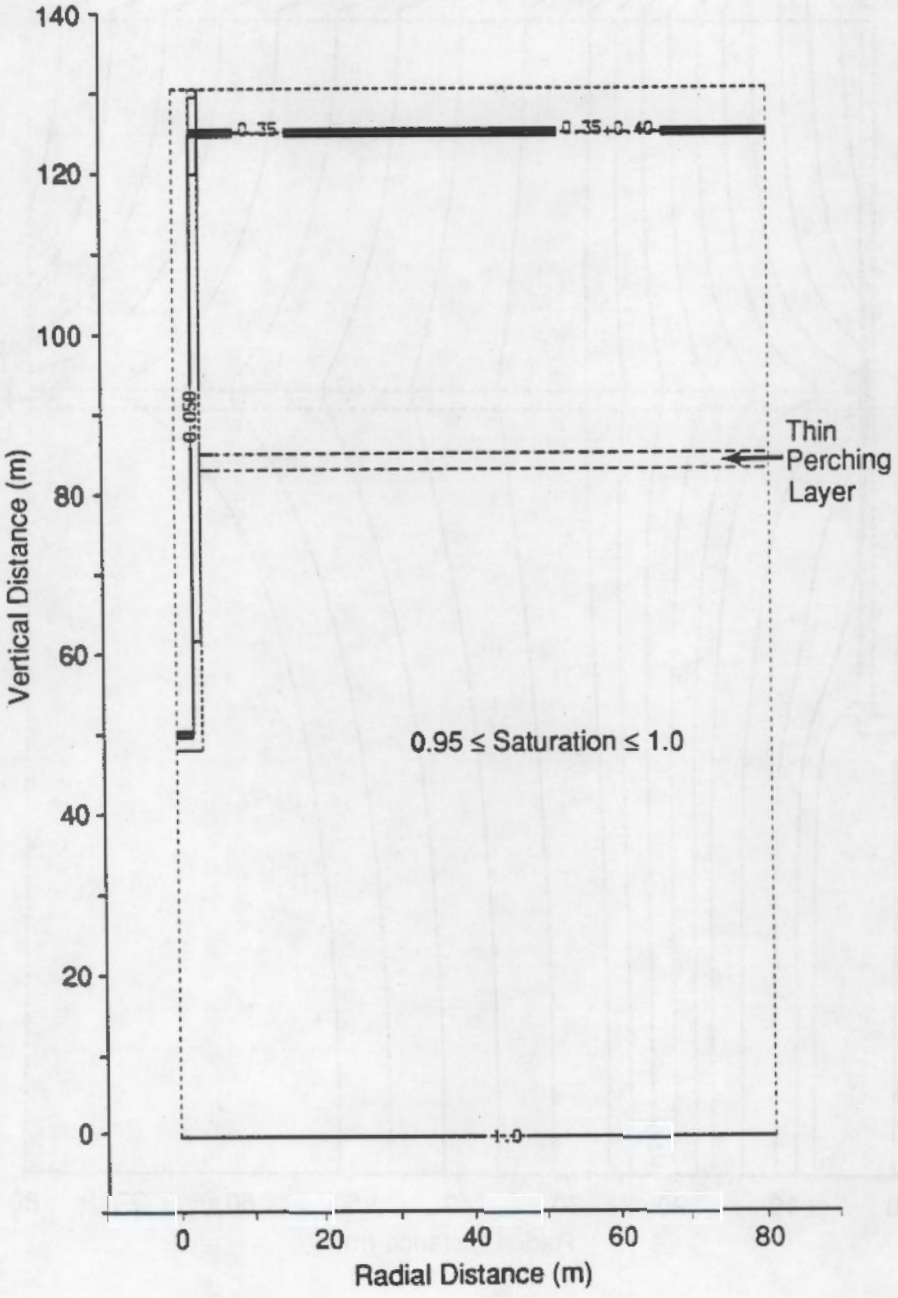

FIGURE 3.11. Saturation Contours for Steady-State Solution of Thin-Perching-Layer Case

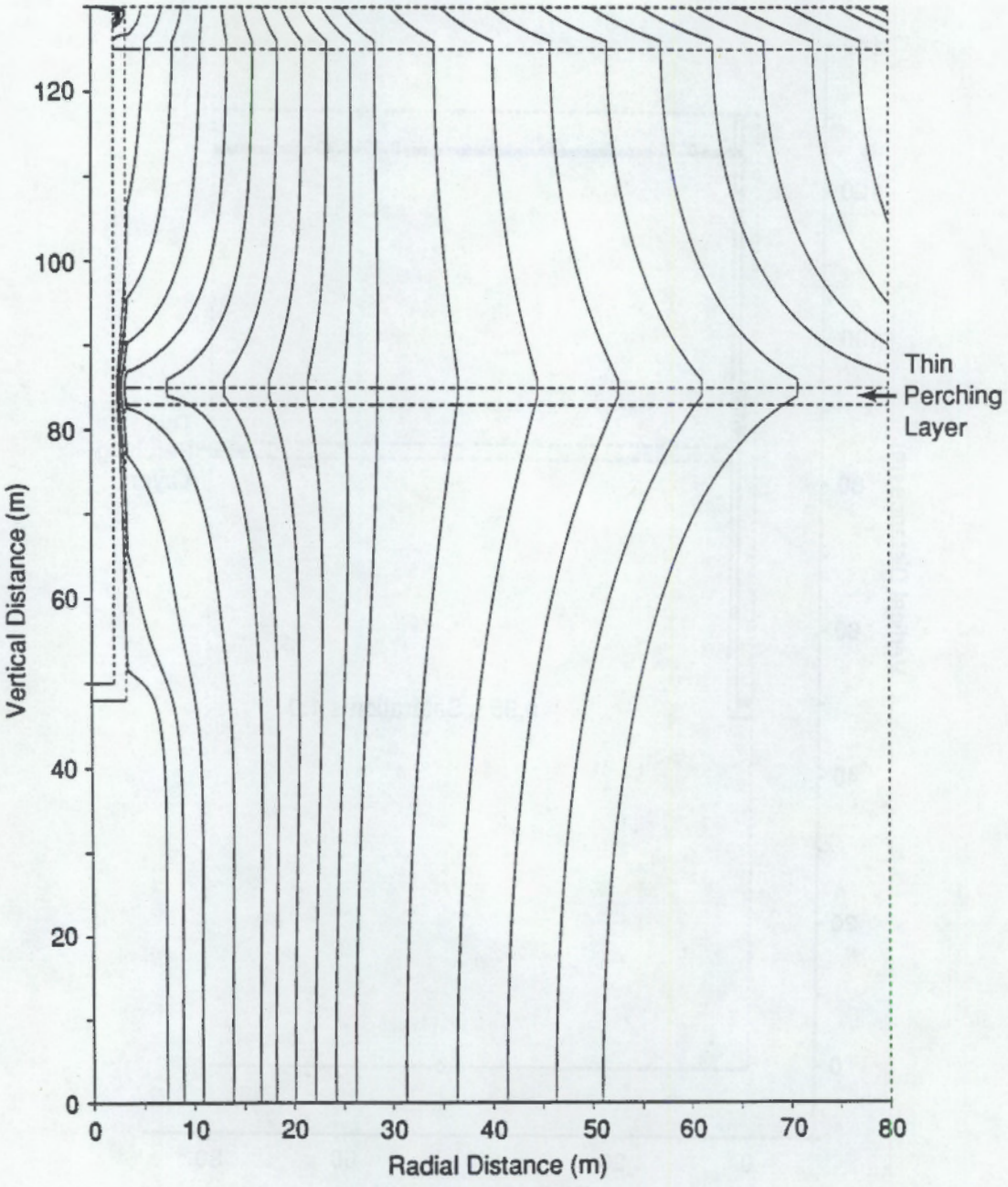

FIGURE 3.12. Streamlines for Thin-Perching-Layer Case

3.1.5 Low-Alpha Case

The low-alpha case is identical to the base case, except that the value of the van Genuchten (1980) curve-fitting parameter, α, is decreased by a factor of 100 for the shaft backfill material. The physical consequence of this is to raise the air-entry potential of the backfill material, allowing more water to enter the shaft than is nominally expected. The differences in the model results were dramatic, as the shaft no longer excluded flow but, rather, functions as a drain for a large radial area. The hydraulic-head contours for the low-alpha case solution, shown in Figure 3.13, are more vertical than horizontal in the vicinity of the shaft and MPZ. The flow regime is perturbed significantly, up to approximately 40 m, from the center of the shaft. The saturation contours, shown in Figure 3.14, are not noticeably different than the base case, except for the range of saturations inside the backfilled shaft. The differences in the streamlines, depicted in Figure 3.15, are substantial compared to the base case. Even at the expected recharge rate (0.1 mm yr^{-1}), the vitric layer functions as a horizontal preferential flow path. More important, the backfilled shaft itself becomes a significant vertical preferential flow path. The combined effect is to decrease travel time over a large radius centered on the shaft. The results of this case make it clear that the air-entry potential of the backfill material must be characterized, and that backfill material must be specified or selected, in part, based on air-entry potential to meet the objectives of shaft backfilling and sealing.

3.1.6 Shaft-Water-Release Case

The results of a hypothetical water release into the backfilled shaft above the CHn unit were predicted by repeating the base case (see Section 3.1.1) with a high-recharge rate imposed at the upper boundary of the backfilled shaft. The recharge rate was assumed equal to one-half the saturated conductivity of the backfill material, or 43.86 m yr^{-1}, which is more than 400 times the expected recharge rate for the base case. Further, the 0.01α condition was assumed for this simulation. This case was designed to determine the extent to which the surrounding CHn unit would imbibe increased flow through the shaft.

Hydraulic-head contours, based on the steady-state solution of the shaft-water-release case, are shown in Figure 3.16, and the saturation contours are shown in Figure 3.17. The saturation contours best illustrate the predicted response of the flow system during a large water release down the shaft. A region of saturation occurs near the lower portion of the shaft as in the high-recharge case, while much of the water is directed horizontally in the vitric unit and exits the model because of the prescribed-head boundary condition. The vitric unit in this case reverses its previous behavior, acting as a preferential flow path away from the shaft rather than toward the shaft, as seen in the saturation contours in the vitric layer in Figure 3.17. These results suggest that the preferential flow path formed by the vitric unit may act beneficially in a shaft-water-release event, routing water away from the shaft to regions where it must then transit the full thickness of the zeolitic unit.

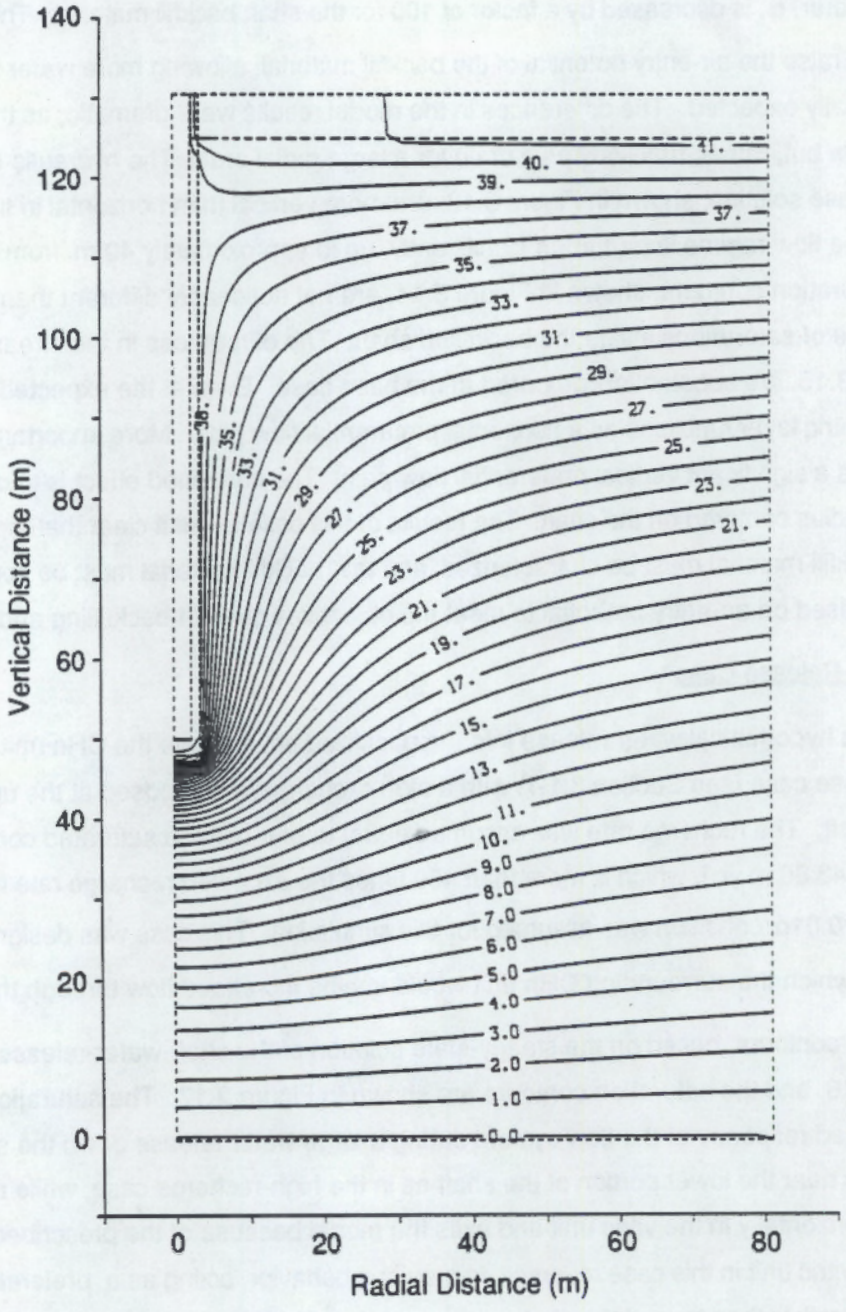

FIGURE 3.13. Hydraulic-Head Contours for Steady-State Solution of Low-Alpha Case

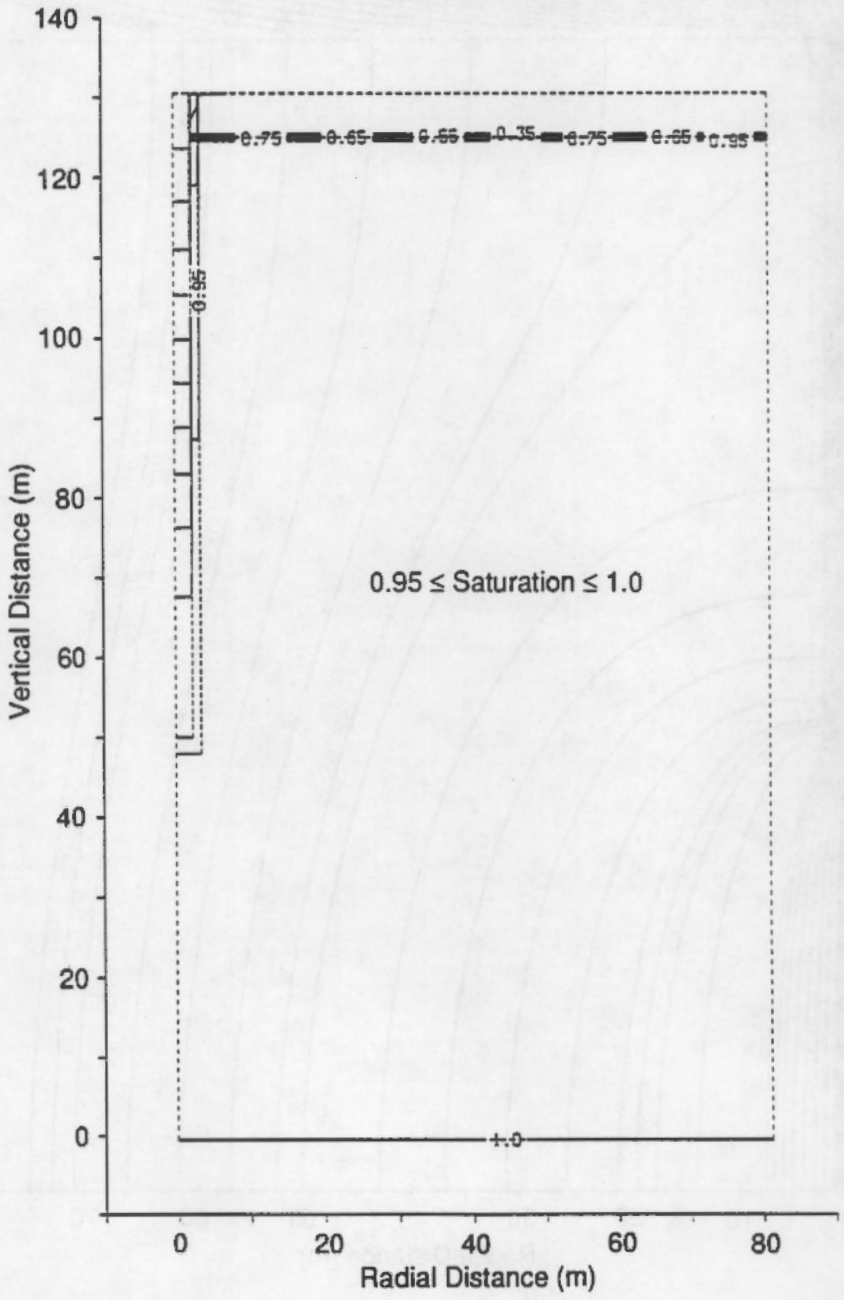

FIGURE 3.14. Saturation Contours for Steady-State Solution of Low-Alpha Case

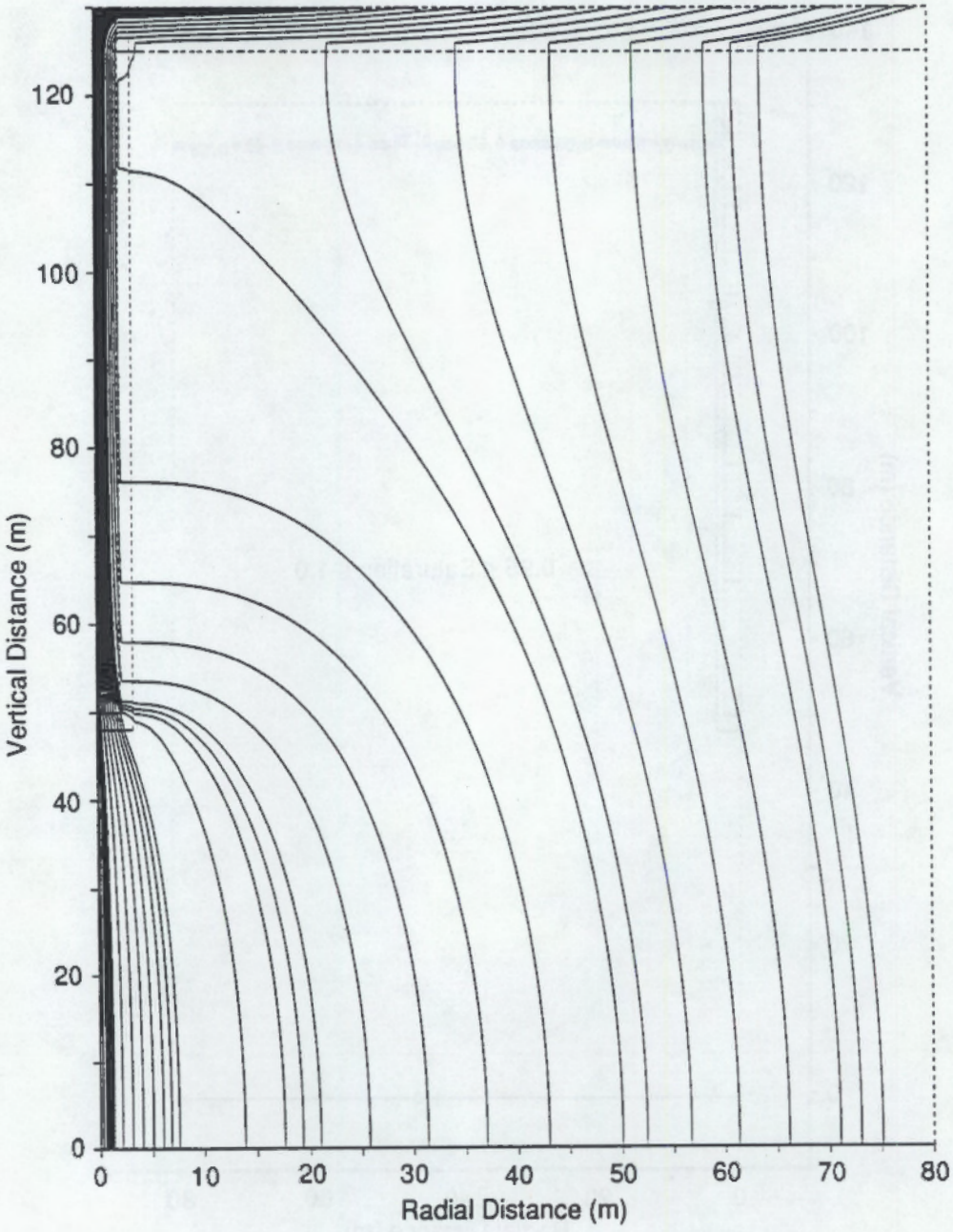

FIGURE 3.15. Streamlines for Low-Alpha Case

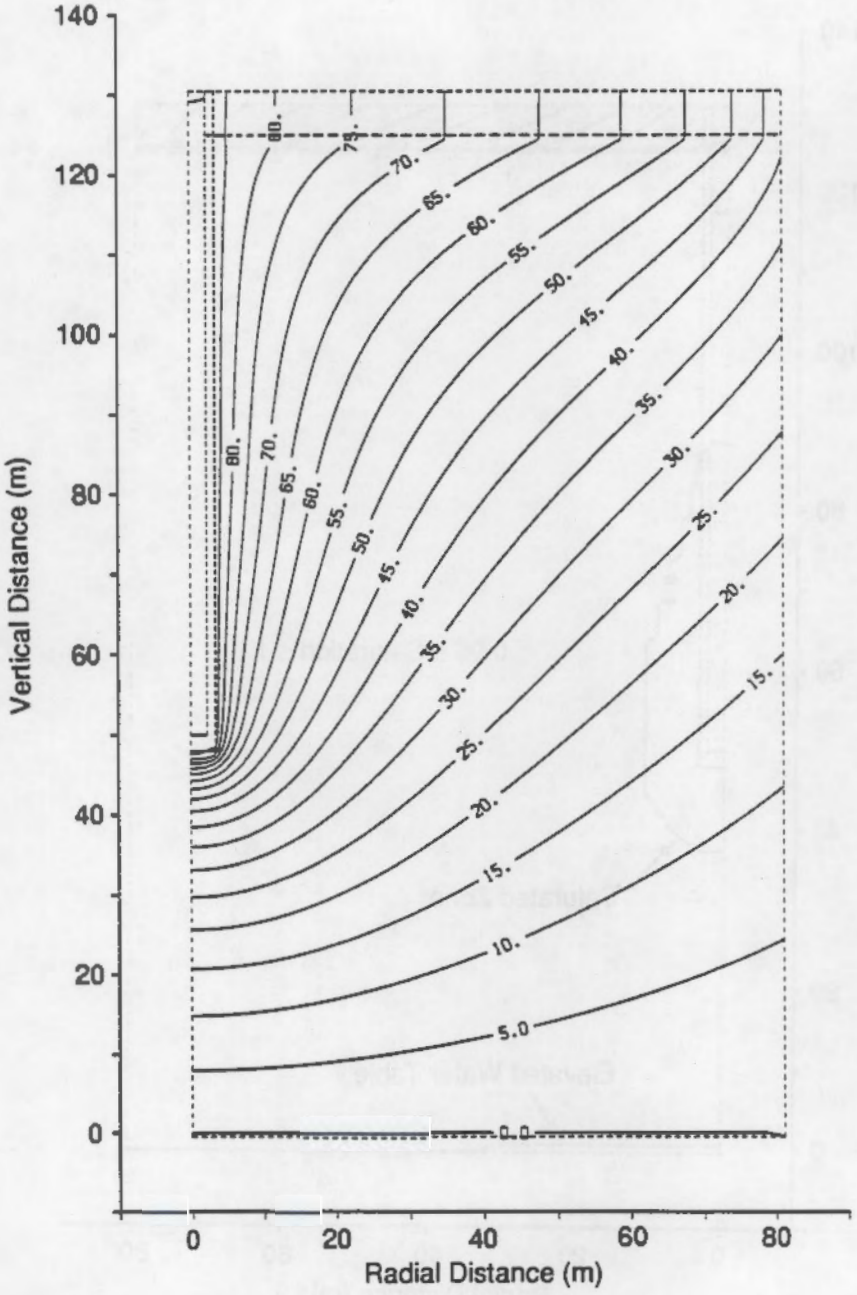

FIGURE 3.16. Hydraulic-Head Contours for Steady-State Solution of Shaft-Water-Release Case

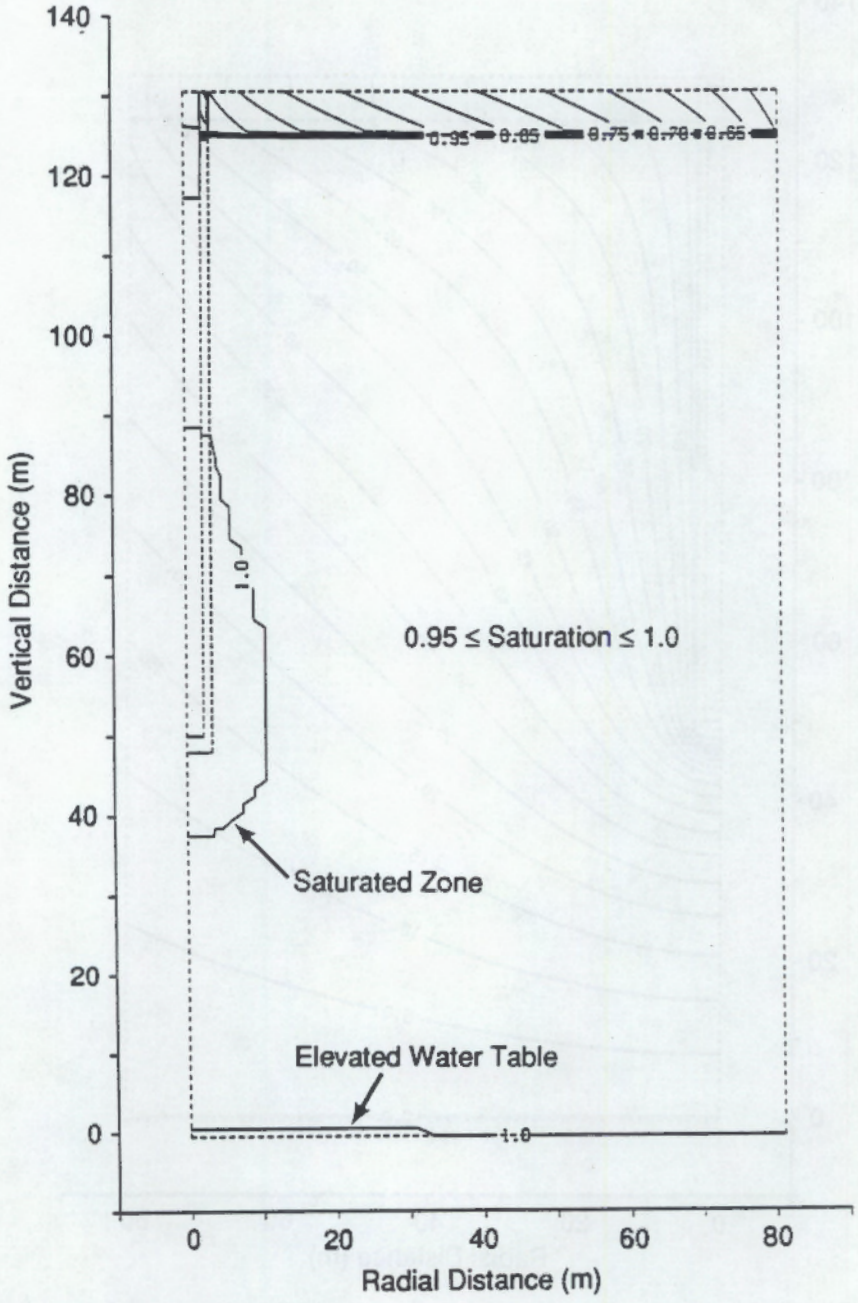

FIGURE 3.17. Saturation Contours for Steady-State Solution of Shaft-Water-Release Case

3.2 COMPARISON OF PREDICTED UNSATURATED ZONE TRAVEL TIMES

One way to assess the impact of the presence of the backfilled shaft in the CHn unit is through comparison of the travel times in the affected radius to the travel times for corresponding undisturbed conditions. To obtain a relative measure, the ratio of disturbed to undisturbed travel times can be used. If there is no effect on travel time, this ratio would equal one. On the other hand, values of this ratio less than one would indicate comparatively shorter travel times and, consequently, greater water movement through this portion of the unsaturated zone. Values greater than one are also possible, where the streamline distance is increased by the horizontal velocity components induced by the presence of the backfilled shaft and the MPZ, and where the vertical velocity components are not of large enough magnitude to compensate. The "overshoot" of the 80-m model in Figure 2.7, in which the travel-time function exceeds the undisturbed travel time in the 60-m radius proximity, is an example of a case where this ratio exceeds one.

Because the impact on travel time varies with radial distance from the shaft, a single value of the disturbed to undisturbed travel-time ratio is meaningless. Instead, the range of values is indicated graphically to show both the relative impact with radial distance and the differences between the cases examined.

Figure 3.18 shows the range of the disturbed-undisturbed travel-time ratio over the 80-m model radius for five cases: base, high recharge, thin perching layer, no vitric, and low alpha. Because the ratio represents a normalized travel time (relative to the corresponding undisturbed case), different traces of the travel-time ratio can be directly compared. Several observations with regard to these traces are worth noting. First, not including the vitric unit in the model gave travel times very similar to the base case for these conditions. Second, the high-recharge rate increased the radius of influence compared to the base case. Third, the presence of the thin perching layer served to increase the horizontal component of the streamline lengths, which in turn resulted in a zone of increased travel time. Finally, the use of a lower alpha for the backfill leads to a much different spatial distribution of travel times and a much larger radius of influence by the shaft and MPZ. The overall effect of the spatial distribution of travel time will be examined in the following section through the use of outflow arrival curves, which integrate the total volumetric flow in the modeled area in both time and space.

The minimum disturbed travel time occurs at the radius where the disturbed-undisturbed travel-time ratio is lowest. Table 3.1 lists the undisturbed travel time and the minimum disturbed travel times for the base, high-recharge, no-vitric, thin-perching-layer, and low-alpha cases. The shaft-water-release case was performed to examine flow response, rather than travel-time effects, and is, therefore, not included in Table 3.1. The reduction in travel times ranges from 58.1% to 83.1%, an impact that is very important if performance of a natural barrier is measured in terms of the minimum travel time. Regulations specified in 10 CFR 60.113 and 10 CFR 960.5-2-1 require that ground-water travel time along the fastest path of likely

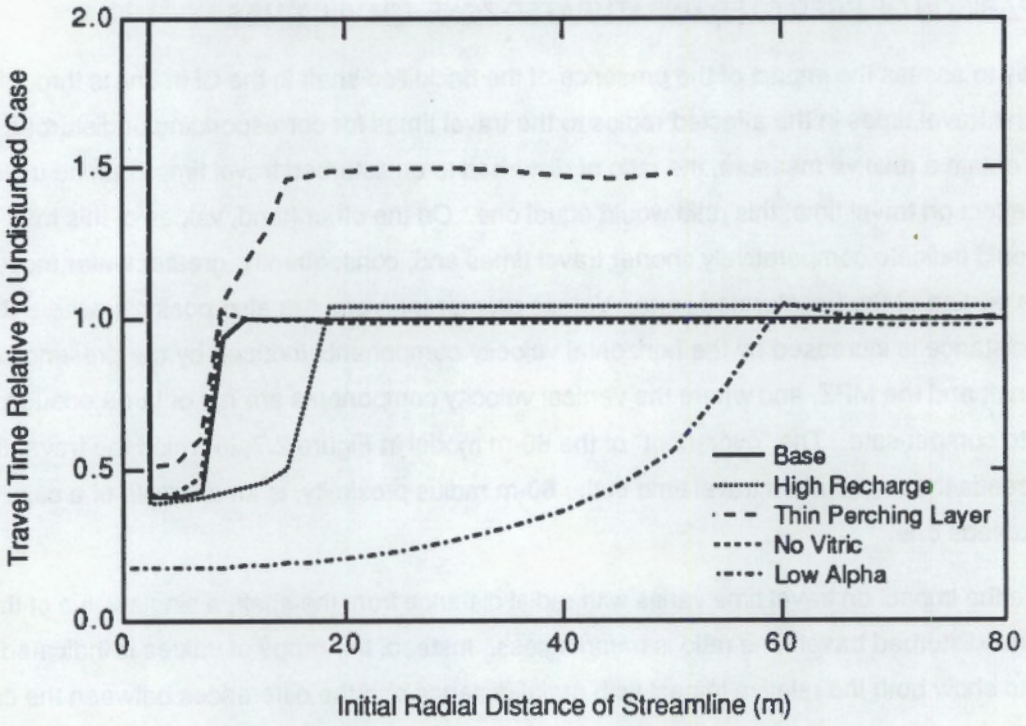

FIGURE 3.18. Travel Time as a Function of Radial Distance for Five Modeling Cases

TABLE 3.1. Predicted Values of Undisturbed and Minimum-Disturbed Travel Time

Case	Undisturbed Travel Time (yr)	Minimum-Disturbed Travel Time (yr)	Reduction
Base	313,100	129,500	58.6%
High Recharge	109,900	42,530	61.3%
No Vitric	313,100	130,700	58.3%
Thin Perching Layer	313,100	56,040	73.1%
Low Alpha	313,100	53,030	83.1%

radionuclide travel from the disturbed zone to the accessible environment shall be at least 1000 yr. The minimum travel time predicted in any case simulated for this analysis was 42,530 yr, which is well above the regulatory limit.

3.3 OUTFLOW ARRIVAL CURVES

In addition to the travel-time comparisons between disturbed and undisturbed conditions, we considered another measure of impact, represented by outflow arrival curves. The outflow arrival curve is a graph of the volume of water per unit time for the 80-m radius model as a function of arrival time at the lower boundary of the model (Nelson 1978, 1981). Conceptually, the outflow arrival curve represents the total outflow rate at the lower boundary that started as a uniform flux at the upper boundary and was tracked from its start at time zero. In the undisturbed, horizontally homogeneous case, this is a uniform flux that is represented graphically as a step function. The height of the step function is equal to the uniform flux rate at the upper boundary and is located at the time equal to the undisturbed travel time for the model domain. Outflow arrival curves, as defined here, are not contaminant arrival curves, though similar curves can be prepared for contaminant-transport simulations.

The outflow arrival curves were prepared by relating outflow versus radial distance information with travel-time versus outflow radius information to obtain outflow versus travel-time results. To produce the outflow arrival curve, the flux rates at the lower boundary are summed with respect to travel time. The summed flux rates are then converted to a volumetric flow rate by multiplying the flux for each computational grid node on the outflow boundary by the outflow area for that node. For this model, these nodal areas are bounded by concentric circles located half-way between successive nodes. Summing the nodal flow rates at a given time then yields the desired outflow arrival curve.

The outflow arrival curve for the disturbed base case, with a single shaft and MPZ, is plotted in Figure 3.19 (dashed line), and is contrasted with the outflow arrival curve predicted for the corresponding undisturbed, steady-state case (solid line). This graph shows that the presence of the exploratory shaft is predicted to cause a very small portion of the water in the 80-m radius area that was modeled to arrive sooner than in the undisturbed case, while a greater portion would arrive later. The outflow arrival curve for the high-recharge case is plotted in Figure 3.20, and shows, in contrast to the base case in Figure 3.19, both the shorter arrival time (caused by high-recharge rate) and the much larger volume of water involved (three times the base case recharge rate). The outflow arrival curve for the no-vitric case is plotted in Figure 3.21. Without the relatively high-conductivity vitric layer, the outflow arrival curve for the single-shaft model is closer to the corresponding one-dimensional undisturbed case than for the base case described above. Finally, Figure 3.22 shows the outflow arrival curve for the low-alpha case. The low-alpha outflow arrival curve shows the greatest impact of all cases examined. A large portion of water arrives sooner than in the corresponding undisturbed solution, and a smaller portion arrives later. The vertical

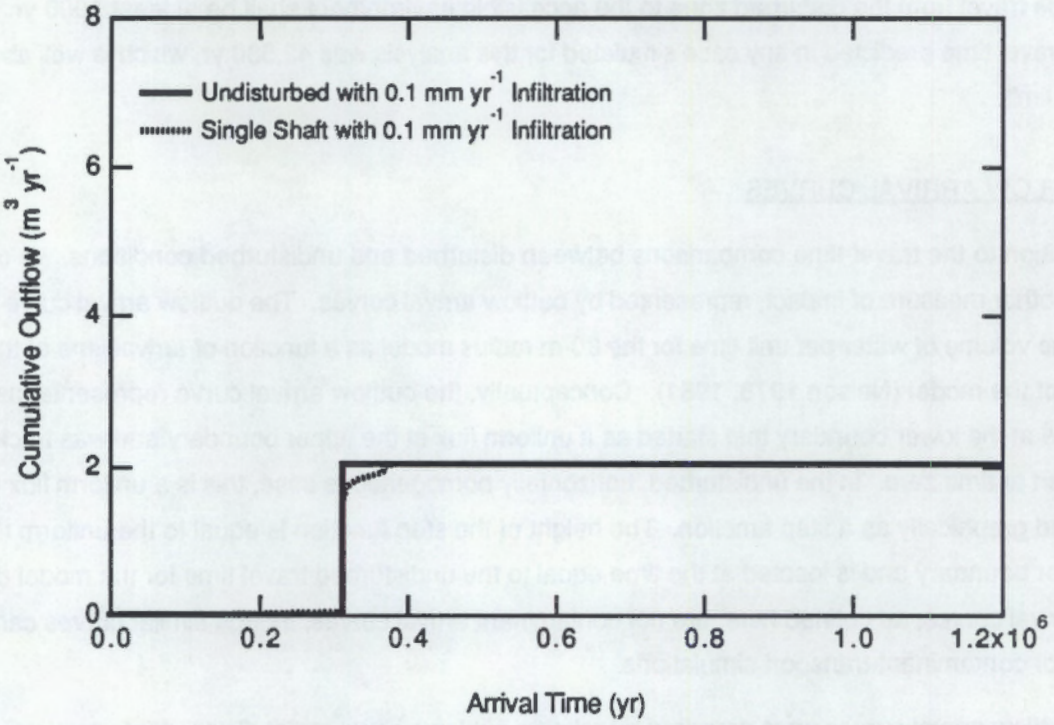

FIGURE 3.19. Outflow Arrival Curves for the Base Case

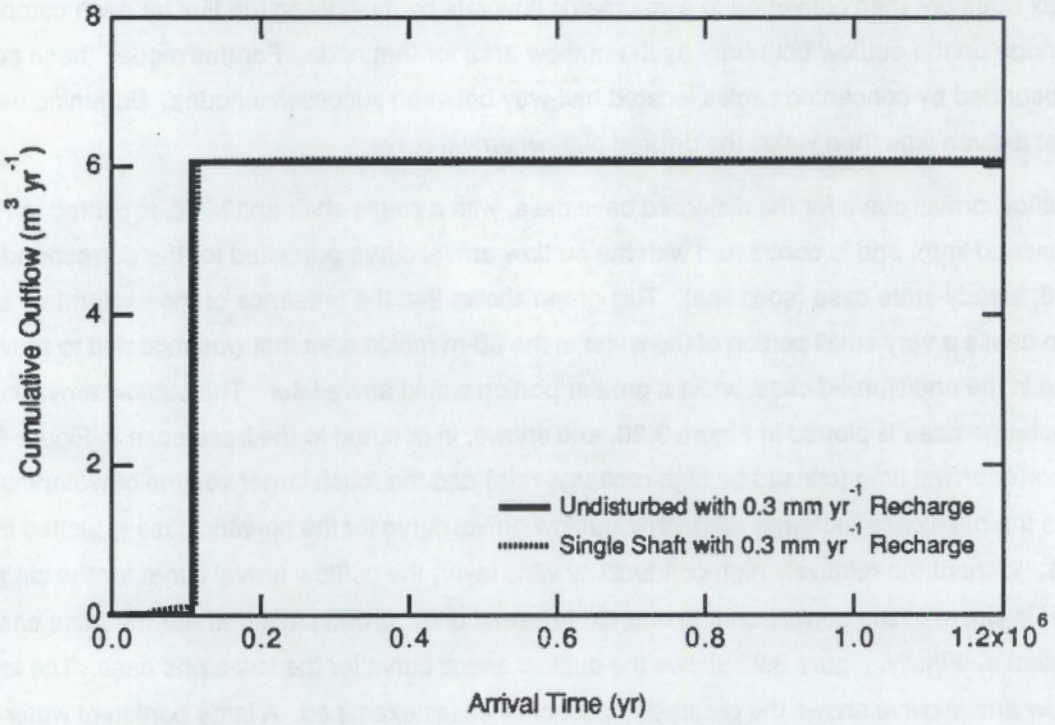

FIGURE 3.20. Outflow Arrival Curves for the High-Recharge Case

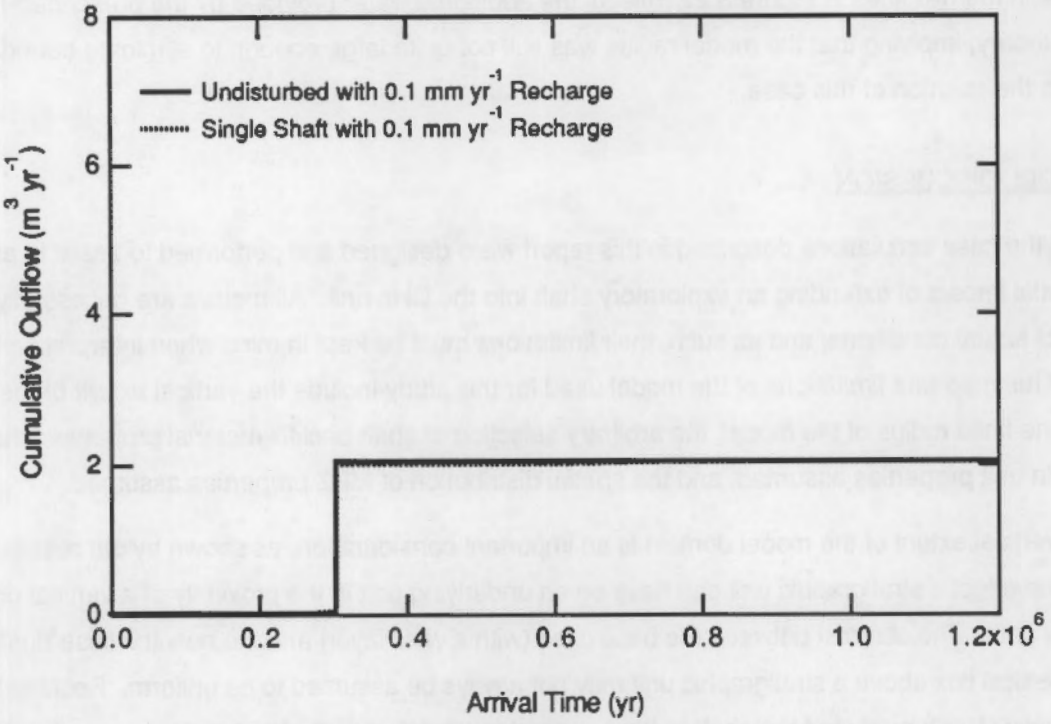

FIGURE 3.21. Outflow Arrival Curves for the No-Vitric Case

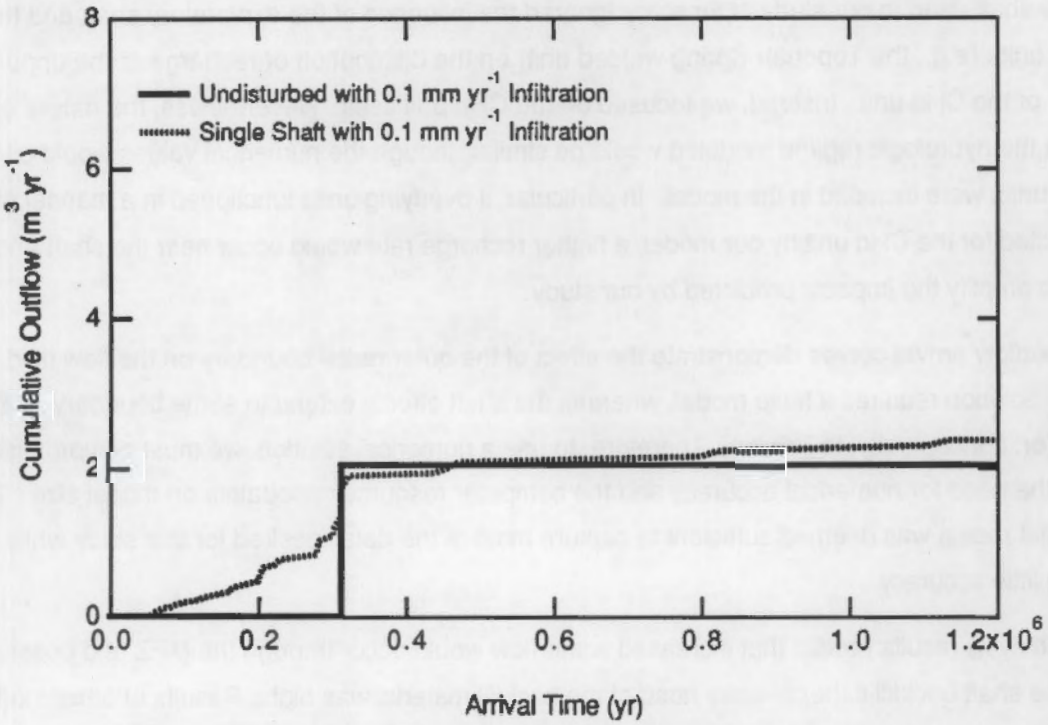

FIGURE 3.22. Outflow Arrival Curves for the Low-Alpha Case

difference in the two lines in Figure 3.22 reflects the additional water provided by the prescribed-head outer boundary, implying that the model radius was still not quite large enough to eliminate boundary effects on the solution of this case.

3.4 MODEL DISCUSSION

All of the case simulations described in this report were designed and performed to assist in assessing the potential impact of extending an exploratory shaft into the CHn unit. All models are necessarily approximations of actual conditions, and as such, their limitations must be kept in mind when interpreting the results. The important limitations of the model used for this study include the vertical extent of the model domain, the finite radius of the model, the arbitrary selection of shaft backfill material properties, the values of the CHn unit properties assumed, and the spatial distribution of MPZ properties assumed.

The vertical extent of the model domain is an important consideration, as shown by our results that indicate the effect a stratigraphic unit can have on an underlying unit in the proximity of a vertical preferential flow path. The contrast between the base case (with a vitric layer) and the no-vitric case illustrates that the vertical flux above a stratigraphic unit may not always be assumed to be uniform. Rockhold, Sagar, and Connelly (1990) predicted the shaft to have a greater impact near the land surface than at depth. They based this prediction on their three-dimensional model of the entire Yucca Mountain stratigraphy, which used a linear approximation feature to represent exploratory shafts, rather than the explicit description of the shaft used in our study. Our study ignored the influence of the exploratory shaft and the overlying units (e.g., the Topopah Spring welded unit) on the distribution of recharge at the upper boundary of the CHn unit. Instead, we focused on the CHn unit itself. Nevertheless, the nature of the impact on the hydrologic regime modeled would be similar, though the numerical values would differ if the overlying units were included in the model. In particular, if overlying units functioned in a manner similar to that predicted for the CHn unit by our model, a higher recharge rate would occur near the shaft and MPZ and would amplify the impacts predicted by our study.

The outflow arrival curves demonstrate the effect of the outer radial boundary on the flow field. A numerical solution requires a finite model, whereas the shaft effects extend to some boundary at a great distance (or, conceptually, to infinity). Therefore, to use a numerical solution, we must compromise between the need for numerical accuracy and the computer resource constraints on model size. The 80-m-model radius was deemed sufficient to capture most of the detail desired for this study while sacrificing little accuracy.

Our analysis results predict that increased water flow would occur through the MPZ and possibly through the shaft backfill if the air-entry head of the backfill material was high. Results of other models of the shaft backfill for the potential repository (Freshley, Dove, and Fernandez 1985) demonstrated that the backfill materials behave as a capillary barrier to water flow. The behavior of the backfill materials is strongly

strongly influenced by the hydraulic properties relative to those of the surrounding media and the recharge rate through Yucca Mountain. The properties of the backfill material can be controlled through selection of materials with specified hydraulic properties. Our model, therefore, represents the flow field near the exploratory shaft for only two possible designs (corresponding to values chosen for α).

The physical and hydraulic properties used in our analyses to represent the vitric and zeolitic layers of the CHn unit are from the literature (Peters et al. 1984; Montazer and Wilson 1984). These values are based on a limited number of samples from boreholes USW-G4 and USW-GU3 that represent our current understanding of the subsurface hydrology at Yucca Mountain.

Finally, as shown by Case and Kelsall (1987), the hydraulic conductivity in the MPZ surrounding a shaft is not uniform. Rather, the increase in hydraulic conductivity is a function of distance from the shaft and decreases exponentially with distance as it approaches the undisturbed conductivity. Our model applied a uniform, average value for the MPZ's conductivity to approximate the increased permeability. One consequence of our constant-value assumption about the MPZ properties is that the continuous variation of properties across the MPZ is modeled as an abrupt change. This results in a somewhat different physical model because of the abrupt change in properties at the interface between the MPZ and the undisturbed rock. For example, the abrupt contrast in air-entry potentials across this interface, as represented in our model, may lead us to predict that water is precluded from the MPZ when, in reality, it is not. An exponentially changing hydraulic conductivity distribution imposed on our model would result in much higher values of hydraulic conductivity in the vicinity of the shaft wall; however, values in the vicinity of the MPZ interface with the undisturbed rock would be virtually that of the undisturbed rock. In reality, there is no interface between the MPZ and the undisturbed rock; rather, it forms a continuum. The consequence of imposing the exponential relationship between MPZ conductivity and radial distance would be that water reaching the shaft wall vicinity would move more rapidly than we predicted, but movement between undisturbed rock and the shaft wall may be slower. The overall impact of such a model refinement is unresolved.

4.0 CONCLUSIONS

The results of this study suggest that the exploratory shaft and MPZ will influence the unsaturated flow field in the CHn unit near these features. In general, the MPZ will locally reduce the minimum travel time for water to transit the CHn unit to the regional water table by at least 58% under expected conditions. These results are illustrated in the contour plots of hydraulic head, saturation, and streamlines. For a recharge rate of 0.3 mm yr^{-1}, which is three times higher than the expected rate for the CHn unit, the effect is similar.

Simulation results are strongly influenced by the hydraulic properties assumed to represent the shaft backfill. To form a capillary barrier to water flow, the conceptual design calls for backfilling shafts with a coarse material, such as crushed tuff. For our simulations, the backfill material properties were approximated using the properties of a gravelly sand. Under certain conditions, such as higher recharge flux or contrasting layer properties, water may be diverted toward the shaft and MPZ. If the backfill material has a significantly lower air-entry potential, the impact of the shaft on the surrounding flow field is much larger than for expected values of air-entry potential. Because selection of backfill properties strongly influences the behavior of the flow system, backfill materials can and should be selected in designing these facilities to minimize water flow into shafts and drifts.

The simulation results also indicate that the effects of the shaft and MPZ are restricted to an approximate 40-m radius, and should not exceed an 80-m radius, which represents an area of 20,106 m^2 in the horizontal plane. Current plans for the potential repository indicate that the underground facility will cover approximately 1380 acres (DOE 1988b), or 5,600,000 m^2. Therefore, the potential area impacted by an exploratory shaft and its radius of influence in the CHn unit is equal to only 0.36% of the total area for the potential repository. To avoid impacts altogether, the exploratory shaft could be located outside, but adjacent to, the sphere of influence of the potential repository. This would provide the characterization data without compromising the integrity of the CHn unit beneath and downgradient of the repository.

Heterogeneities in the form of thin layers of higher and lower permeability materials will influence the unsaturated flow field near the exploratory shaft and MPZ. Comparison of simulation results for a case with both the vitric and zeolitic layers of the CHn unit to results for a case that included only the zeolitic layer demonstrates that the presence of the vitric layer decreases travel time in the presence of a shaft and MPZ. When the relatively high-conductivity vitric layer is present, flow is channeled in that layer toward the exploratory shaft. The presence of the vitric layer reduces the minimum travel time only a small amount in comparison to the base case simulation. In the low-alpha case, however, this heterogeneity is much more important. The boundary conditions employed in the simulation prevented the occurrence of a saturated

zone in the thin-perching-layer case; however, the presence of a lower permeability layer was shown to divert water laterally. From our results, we conclude that the impact of the shaft and MPZ will depend on the actual heterogeneities present in the CHn unit.

The purpose of our study has been to quantify the negative impacts on site performance of seeking a greater knowledge of the CHn unit. Qualitatively, we have shown that expected values of travel time through the CHn unit, which now range in the hundreds of thousands of years, may be compromised and, at worst, would range in the tens of thousands of years. All estimates exceed 1000 yr, the minimum travel time required by regulations, by a factor of 40 or higher. The positive impacts gained through sampling and study of the CHn unit were not considered. The parameters of importance for site characterization have been shown to include the recharge rate and the effective hydraulic properties of the formations, MPZ, and backfill material and their ranges of variability. It is also important to identify any thin layers with contrasting physical and hydraulic properties that may be present within the CHn unit because of the hydrologic importance such layers have in the vicinity of a shaft.

5.0 REFERENCES

10 CFR 60. 1987. U.S. Nuclear Regulatory Commission, "Disposal of High-Level Radioactive Wastes in Geologic Repositories." U.S. Code of Federal Regulations.

10 CFR 960. 1987. U.S. Nuclear Regulatory Commission, "General Guidelines for the Recommendation of Sites for Nuclear Waste Repositories." U.S. Code of Federal Regulations.

Case, J. B., and P. C. Kelsall. 1987. Modification of Rock Mass Permeability in the Zone Surrounding a Shaft in Fractured, Welded Tuff. SAND86-7001, Sandia National Laboratories, Albuquerque, New Mexico.

DOE (U.S. Department of Energy). 1988a. Site Characterization Plan, Yucca Mountain Site, Nevada Research and Development Area, Nevada. DOE/RW-0199, Volume II, Part A, Office of Civilian Radioactive Waste Management, Washington, D.C.

DOE (U.S. Department of Energy). 1988b. Site Characterization Plan, Overview, Yucca Mountain Site, Nevada Research and Development Area, Nevada. DOE/RW-0198, Office of Civilian Radioactive Waste Management, Washington, D.C.

Fernandez, J. A., and M. D. Freshley. 1984. Repository Sealing Concepts for the Nevada Nuclear Waste Storage Investigations Project. SAND83-1778, Sandia National Laboratories, Albuquerque, New Mexico.

Fernandez, J. A., T. E. Hinkebein, and J. B. Case. 1989. Selected Analyses to Evaluate the Effect of the Exploratory Shafts on Repository Performance at Yucca Mountain. SAND85-0598, Sandia National Laboratories, Albuquerque, New Mexico.

Freshley, M. D., F. H. Dove, and J. A. Fernandez. 1985. Hydrologic Calculations to Evaluate Backfilling Shafts and Drifts for a Prospective Nuclear Waste Repository in Unsaturated Tuff. SAND83-2465, Sandia National Laboratories, Albuquerque, New Mexico.

Montazer, P., and W. E. Wilson. 1984. Conceptual Hydrologic Model of Flow in the Unsaturated Zone, Yucca Mountain, Nevada. Water-Resources Investigations Report 84-4345, U.S. Geological Survey, Denver, Colorado.

Mualem, Y. 1976. A Catalogue of the Hydraulic Properties of Unsaturated Soils. Technion Israel Institute of Technology, Haifa, Israel, p. 85.

Nelson, R. W. 1978. "Evaluating the Environmental Consequences of Groundwater Contamination. 2. Obtaining Location/Arrival Time and Location/Outflow Quantity Distributions for Steady Flow Systems." Water Resour. Res. 14(3):416-428.

Nelson, R. W. 1981. Assessment of Effectiveness of Geologic Isolation Systems. Use of Geohydrologic Response Functions in the Assessment of Deep Nuclear Waste Repositories. PNL-3817, Pacific Northwest Laboratory, Richland, Washington.

Peters, R. R., E. A. Klavetter, I. J. Hall, S. C. Blair, P. H. Heller, and G. W. Gee. 1984. Fracture and Matrix Hydrologic Characteristics of Tuffaceous Materials from Yucca Mountain, Nye County, Nevada. SAND84-1471, Sandia National Laboratories, Albuquerque, New Mexico.

Rockhold, M. L., B. Sagar, and M. P. Connelly. 1990. "Multi-Dimensional Modeling of Unsaturated Flow in the Vicinity of Exploratory Shafts and Fault Zones at Yucca Mountain, Nevada," in High Level Radioactive Waste Management.Vol. 2: Proceedings of the International Topical Meeting, Las Vegas, Nevada, April 8-12, 1990. American Nuclear Society, Inc., La Grange Park, Illinois, pp. 1192-1199.

Runchal, A. K., and B. Sagar. 1989. PORFLO-3: A Mathematical Model for Fluid Flow, Heat, and Mass Transport in Variably Saturated Geologic Media, Users Manual, Version 1.0. WHC-EP-0041, Westinghouse Hanford Company, Richland, Washington.

Sagar, B., and A. K. Runchal. 1990. PORFLO-3: A Mathematical Model for Fluid Flow, Heat, and Mass Transport in Variably Saturated Geologic Media, Theory and Numerical Methods, Version 1.0. WHC-EP-0042, Westinghouse Hanford Company, Richland, Washington.

van Genuchten, M. T. 1980. "A Closed Form Equation for Predicting the Hydraulic Conductivity of Unsaturated Soils." Soil Sci. Soc. Am. J. 44:982-998.

Williams, R. E., S. D. Vincent, and G. Bloomsburg. 1990. "Hydrogeologic Impacts of Mine Design in Unsaturated Rock." Mining Engineering, October:1177-1183.

Worsey, P. N. 1985. "In Situ Measurement of Blast Damage Underground by Seismic Refraction Surveys." Proceedings of the 26th U.S. Symposium on Rock Mechanics, Rapid City, South Dakota, pp. 1133-1140.

PNL-7648
UC-802

DISTRIBUTION

No. of Copies

OFFSITE

2 DOE Office of Scientific and Technical Information

C. P. Gertz, Associate Director
Office of Geologic Disposal, RW-20
Yucca Mountain Site Characterization Project Office
101 Convention Center Drive
Phase 2, Suite 200
Las Vegas, NV 89109

J. J. Lorenz
U.S. Department of Energy
Yucca Mountain Site Characterization Project Office, M/S 523
P.O. Box 98608
Las Vegas, NV 89193-8608

J. R. Dyer
U.S. Department of Energy
Yucca Mountain Site Characterization Project Office, M/S 523
P.O. Box 98608
Las Vegas, NV 89193-8608

No. of Copies

ONSITE

2 DOE Richland Operations Office

D. C. Langstaff
J. J. Sutey

33 Pacific Northwest Laboratory

M. P. Bergeron
P. G. Doctor
R. M. Ecker
P. W. Eslinger
J. W. Falco
M. D. Freshley (2)
J. M. Hales
C. K. Hastings (2)
P. C. Hays
B. V. Johnston
C. T. Kincaid
M. R. Kreiter
M. A. McGraw
R. W. Nelson
W. E. Nichols (5)
M. L. Rockhold (2)
R. L. Skaggs
J. L. Smoot
V. R. Vermeul
S. K. Wurstner
Publishing Coordination
Technical Report Files (5)